

Rochester Institute of Technology

RIT Scholar Works

Theses

5-8-2019

An Investigation of Chipping Generation and Propagation on Carbide Tool under Various Cutting Conditions in End Milling of Low Carbon Steel

Shuhuan Zhang
sz7199@rit.edu

Follow this and additional works at: <https://scholarworks.rit.edu/theses>

Recommended Citation

Zhang, Shuhuan, "An Investigation of Chipping Generation and Propagation on Carbide Tool under Various Cutting Conditions in End Milling of Low Carbon Steel" (2019). Thesis. Rochester Institute of Technology. Accessed from

This Thesis is brought to you for free and open access by RIT Scholar Works. It has been accepted for inclusion in Theses by an authorized administrator of RIT Scholar Works. For more information, please contact ritscholarworks@rit.edu.

ROCHESTER INSTITUTE OF TECHNOLOGY

An Investigation of Chipping Generation and Propagation on Carbide Tool under Various Cutting Conditions in End Milling of Low Carbon Steel

Submitted by

Shuhuan Zhang

A Thesis Submitted in Partial Fulfillment of the Requirements for Master of Science
in Manufacturing and Mechanical Engineering Technology

**Department of Manufacturing and Mechanical Engineering Technology
College of Engineering and Technology**

Approved by:

Dr. Rui Liu

Department of Mechanical Engineering

(Advisor)

Dr. Patricia Iglesias

Department of Mechanical Engineering

(Committee Member)

Dr. Alfonso Fuentes

Department of Mechanical Engineering

(Committee Member)

Prof. Betsy Dell

Department of Manufacturing and
Mechanical Engineering Technology

(Department Representative)

Rochester Institute of Technology

Rochester, New York

05/08/2019

Dedication

I dedicate this thesis to my family for nursing me with affections and love and their dedicated partnership for success in my life.

Acknowledgement

I would initially like to thank my thesis advisor Dr. Rui Liu in the Mechanical Engineering Department at Rochester Institute of Technology. Dr. Liu's office door was always open whenever I ran into trouble spots or had questions about my research project. He is always there to guide me towards the right direction to finish this study independently.

I would also like to acknowledge Dr. Patricia Iglesias, Dr. Alfonso Fuentes, Prof. Betsy Dell, and Mr. Michael Walker served as my thesis reading committee, and I am gratefully indebted to them for their very valuable comments on my thesis work.

I'm also grateful to the experts who were involved in the validation survey for this research project: Mr. Jan Maneti, Mr. Craig Arnold, Mr. Ricky Wurzer, Mr. Sean O'Brien. Without their passionate participation and input, the milling test and measurement could not have been successfully finished.

Abstract

Tool conditions are the essential factors in determining the geometric accuracy and the machined surface quality in the milling process. The different mechanisms of tool condition can be classified as tool wear, chipping, and built-up edge. The chipping, which is one of the decisive tool conditions when the brittle milling tools are used in milling, has not been well investigated by previous studies since the chipping is randomly occurs.

Therefore, the main objective of this study is to comprehensively investigate the generation and propagation of chipping in the milling process. To realize this objective, the carbide milling tools were used to dry cut 1020 low carbon steel with different combinations of cutting speed and chip load. Under each combination, the cutting tool was evaluated in terms of various tool conditions over a certain cutting distance until the milling tool failed.

The result showed that the chipping mainly occurred under the low spindle speed or high chip load per tooth since the cutting force was high. Once the chipping occurred on one flute, other flutes also had the chipping at the same position since the chipping occurred initially increased the chip load per tooth of the next flute. After the chipping was generated, it extended in the following milling process until the width of chipping met the failure criterion. It is found that most of the chipping extended and met the failure criterion in a short cutting distance. However, the chipping which propagated slowly shown three stages with different expansion rates before the end of tool life. Meanwhile, the flank wear was observed on the outline of chipping and was considered as a factor for the chipping propagation since the flank wear increases with the cutting force. The milling test was stopped at the end of tool life, and it was found that the tool life of all the milling tools was shorter than the tool life estimated by using the Taylor equation. However, the Taylor equation only considers the flank wear as a factor for the tool life, whereas, the chipping was

dominated in this study.

Table of Contents

Dedication	i
Acknowledgement	iii
Abstract.....	iv
List of Figures.....	x
List of Tables	xii
Glossary	xiii
Chapter 1 Introduction	1
Chapter 2 Literature Review	5
2.1 Location and shape of chipping	5
2.2 Generation of chipping	5
2.2.1 Mechanical load	6
2.2.2 Cyclic thermal load	6
2.2.3 Combination of high mechanical load and high thermal load	8
2.3 Propagation of chipping.....	9
2.4 Failure criteria	11
Chapter 3 Research Gaps.....	14
Chapter 4 Objectives	15
Chapter 5 Experimental Procedure	16
5.1 Cutting tool, equipment, and workpiece	16
5.1.1 Milling tool	16
5.1.1 Workpiece	16

5.1.2 Milling machine	17
5.2 Cutting conditions	18
5.2.1 Spindle speed (RPM)	18
5.2.2 Chip load per tooth (CLPT)	18
5.2.3 Axial depth of the cut & radial depth of cut	19
5.2.4 Milling process.....	20
5.3 Observation equipment	21
5.3.1 Digital microscope	21
5.3.2 Surface Profilometer	21
5.4 Procedure	24
5.4.1 Initial stage.....	24
5.4.1 Follow-up stage.....	29
Chapter 6 Results & Discussion.....	32
6.1 Chipping behaviors in different tool locations.....	32
6.2 Effects of cutting conditions on chipping	35
6.2.1 High RPM and low chip load.....	35
6.2.2 Low RPM and low chip load	36
6.2.3 Low RPM and high chip load	37
6.3 Chipping propagation among different flutes	39
6.4 Chipping progression in terms of cutting distance	41
6.4.1 The extension of the chipping in long cutting distance	41
6.4.2 The extension of the chipping in short cutting distance	44
6.5 Mutual effect between the tool wear and chipping	47

6.6 Usability of Taylor equation	48
Chapter 7 Conclusions.....	50
Chapter 8 Future Work.....	52
Appendix A: Chemical composition of 1020 steel.....	53
Appendix B: Mechanical properties of 1020 steel.....	54
Appendix C: Cutting conditions used in this study	55
Appendix D: Cutting distance used in each loop	56
Appendix E: Results of observation in initial stage	57
Appendix F-1: Results of observation in the first loop of follow-up stage.....	59
Appendix F-2: Results of observation in the second loop of follow-up stage	61
Appendix F-3: Results of observation in the third loop of follow-up stage	62
Appendix F-4: Results of observation in the forth loop of follow-up stage	63
Appendix F-5: Results of observation in the fifth loop of follow-up stage	64
Appendix F-6: Results of observation in the sixth loop of follow-up stage	65
Appendix F-7: Results of observation in the seventh loop of follow-up stage.....	66
Appendix F-8: Results of observation in the eighth loop of follow-up stage	67
Appendix F-9: Results of observation in the ninth loop of follow-up stage.....	68
Appendix F-10: Results of observation in the tenth loop of follow-up stage.....	69
Appendix F-11: Results of observation in the eleventh loop of follow-up stage.....	70
Appendix F-12: Results of observation in the twelfth loop of follow-up stage.....	71
Appendix F-13: Results of observation in the thirteenth loop of follow-up stage.....	72
Appendix F-14: Results of observation in the fourteenth loop of follow-up stage.....	73
Appendix F-15: Results of observation in the fifteenth loop of follow-up stage	74

Appendix F-16: Results of observation in the sixteenth loop of follow-up stage	75
Appendix G: An example of the map	76
Reference	77

List of Figures

Fig. 1 The location of chipping on the milling tool [6]	5
Fig. 2 The structure of the micro-cracks on the cutting edge [29].....	7
Fig. 3 Comb cracks [26].....	7
Fig. 4 The vertical cracks on the cutting edge [28].....	8
Fig. 5 Tendency of the maximum tool wear [31]	9
Fig. 6 TRACK K3 EMX vertical milling machine.....	17
Fig. 7 (a) High RDOC (b) low RDOC	20
Fig. 8 KLAREN USB Digital Microscope	21
Fig. 9 WYKO NT1100 dynamic profilometer.....	22
Fig. 10 (a) Flank face is reflecting the light to profilometer (b) Wear land is reflecting the light to the profilometer.....	22
Fig. 11 (a) Shape of chipping when the flank face is vertical to the light (b) actual chipping wear land.....	24
Fig. 12 Procedure of the pretest	25
Fig. 13 (a) usable milling tool (b) unusable milling tool	26
Fig. 14 (a) The new cutting zone (b) The cutting zone with flank wear, and the dark blue part is the flank wear (c) The cutting zone with chipping, and the parameters were used to calculate the width of chipping	27
Fig. 15 Map obtained from initial stage.....	29
Fig. 16 Follow-up stage	30
Fig. 17 Three cutting region of the cutting edge.....	32
Fig. 18 The chipping in the corner region of the tool #4	33

Fig. 19 The chipping located on the depth-of-cut region.....	34
Fig. 20 (a) The rake angle is positive when the chip load is reasonable (b) The rake angle is negative when the chip load is low.....	36
Fig. 21 (a) the chipping on the tool #31 after cutting 8 inches of workpiece (b) the chipping on the tool #2 after cutting 8 inches of workpiece.....	37
Fig. 22 (a) the chipping on the tool #2 after cutting 2 inches of workpiece (b) the chipping on the tool #29 after cutting 2 inches of workpiece.....	38
Fig. 23 (a) the fourth flute after cutting 2 inches (b) the first flute after cutting 2 inches (c) the second flute after cutting 2 inches (d) the third flute after cutting 2 inches (e) the fourth flute after cutting 4 inches (f) the first flute after cutting 4 inches (g) the second flute after cutting 4 inches (h) the third flute after cutting 4 inches (i) the fourth flute after cutting 6 inches (j) the first flute after cutting 6 inches (k) the second flute after cutting 6 inches (l) the third flute after cutting 6 inches	40
Fig. 24 The variation of chipping in long cutting distance	41
Fig. 25 (a) Cutting edge without chipping (b) cutting edge with chipping.....	42
Fig. 26 (a) Tool # 24 before the experiment (b) Tool # 24 when cutting distance was 6 inches (c) Tool # 24 when cutting distance was 46 inches (d) Tool # 24 when cutting distance was 72 inches	43
Fig. 27 The variation of chipping in short cutting distance	45
Fig. 28 (a) Tool # 7 when cutting distance was 2 inches (b) Tool # 7 when cutting distance was 4 inches	46
Fig. 29 (a) the chipping on the tool #24 before extending (b) the chipping on the tool#24 after extending.....	48

List of Tables

Table 1. Flank wear used as a failure criterion for tool life.....	3
Table 2. Combined failure criteria.....	12
Table 3. Mechanical properties of the milling tool.....	16

Glossary

PCD	Polycrystalline Diamond
PVD	Physical Vapor Deposition
CVD	Chemical Vapor Deposition
RPM	Round per Minute
CLPT	Chip load per tooth
HRB	Rockwell Hardness Measured on the B Scale
ADOC	Axial Depth of Cut
RDOC	Radial Depth of Cut
BUE	Built-up Edge

Chapter 1 Introduction

Various cutting parameters involved in machining are related to the cutting tool which is a critical component of any machining configurations [1]. The significant indexes which define the quality of the machined part are dimensional accuracy and surface roughness, which are both directly affected by cutting tool conditions [2]. The investigation of different cutting tool conditions is necessary to optimize machining parameters to improve the quality of machined products. However, due to the complexity of the machining process and the low accessibility, the progression of various cutting tool conditions are quite difficult to be observed and monitored during the process to obtain the desired product quality and minimize the machine downtime [3]. Therefore, the prediction of the progression of cutting tool conditions offers an alternative way to investigate tool fail modes and arrange the production plan.

Based on different physical mechanisms and regions, cutting tool conditions can be classified into different categories which differently influence the machined part quality and the cutting tool life. The tool wear is one of the most commonly observed cutting tool conditions, which can be further classified as flank wear and crater wear based on the position [4]. The built-up edge is another type of tool condition which can influence the cutting tool geometry and further affect the dimensional accuracy of machined products [5]. Furthermore, the chipping, which is fundamentally caused by the brittle fracture on the cutting edge [6], is considered as another major cutting tool condition when the brittle cutting tool is used in the successive cutting process [7], such as milling. Research indicates the chipping can also be classified as one type of tool wear [8][9]. Considering different formation mechanisms, the chipping was studied independently from the tool wear in this study. The chipping can largely change the shape of the milling tool edge and

even increase the surface roughness of the machined part and the geometrical accuracy significantly [10]. However, the chipping shape appeared very randomly [11] and the mechanism of chipping involving fracture was still considered as a probabilistic event [12]. Therefore, the chipping generation and propagation on the milling tools still remains an open research question.

The period up to the point when the tool conditions are so serious that the milling tool cannot be used for further cutting operations is considered as the tool life [6], and this point is defined as the tool life criterion. The fixed tool life criterion is primarily used for stopping the experiment and comparative purposes. The typical tool conditions which have been used in the previous studies as tool life criteria include flank wear, crater wear, and chipping.

The flank wear is classified as uniform flank wear, non-uniform flank wear, and localized flank wear in ISO 8688-2: 1989 [6], both the maximum width and average width of these different types of flank wear have been used as criteria which have been listed in Table 1. In addition, the width of flank wear can be used to estimate the tool file. The most commonly used method is Taylor equation which is shown in equation below:

$$VT^n = C \quad (1)$$

where, V is the cutting speed and T is the cutting time which is tool life. The value n and C mainly depend on the material of workpiece, coolant, and the width of flank wear which considered as the criterion of the end of tool life [13]. However, as it is known that the flank wear is the only tool condition considered in the Taylor equation. Therefore, if the Taylor equation can be used or not when other tool conditions, such as chipping, are dominating will be studied.

Table 1. Flank wear used as a failure criterion for tool life.

Reference	Cutting tool material	Failure criteria
Alauddin and Baradie [14]	Solid uncoated, high-speed steel	Average uniform flank wear = 0.012 in or Maximum localized flank wear = 0.020 in
Chakraborty [15]	Coated carbide steel	Maximum flank wear = 0.016 in
Santos et al. [16]	Coated carbide steel	Maximum flank wear = 0.028 in
Alauddin et al. [17]	Carbide steel	Average uniform flank wear = 0.030 in or Average localized flank wear = 0.028 in
Gu et al. [18]	Uncoated carbide steel	Flank wear = 0.004 in
D'Errico [19]	Cermet	Average flank wear = 0.008 in
Diniz and Filho [20]	Carbide steel	Maximum flank wear = 0.028 in
Wang et al. [21]	Cubic boron nitride	Average flank wear = 0.016 in

Except the width of flank wear mention before, the depth of crater wear has also being used as a tool life criterion at high cutting speeds in various milling studies. For example, Kudou et al. [22] used the maximum depth of crater wear at 0.03 mm as the tool life criterion, and the average depth of crater wear was also been considered as a potential criterion of the tool life [23].

Moreover, for successive cutting processes, e.g. milling, the chipping on the cutting edge has been considered as an important failure mode that affects the tool life and the performance of cutting tools made by brittle materials [7], and the width of chipping has usually been used by combined failure criteria in conjunction with the flank wear and the crater wear.

In practical scenarios, the tool life criterion strongly depends on the requirements of the dimensional accuracy or surface quality. However, the failure criteria in ISO and the other failure criteria were defined base on the experience. Therefore, a method to find the reasonable width of

chipping which can be used as the failure criteria in the milling process needs to be studied.

Chapter 2 Literature Review

2.1 Location and shape of chipping

The chipping is jagged on the cutting edges or the cavities and depressions on the flank face of the milling tool [24], which has been shown in Fig. 1. Chipping can be further classified by ISO 8688-2:1989 [6] in three types which are the uniform chipping, non-uniform chipping, and localized chipping. The uniform chipping is jagged with approximately equal size along the cutting edge, the non-uniform chipping is the chipping which concentrates on a small number of random positions on the cutting edges, and the localized chipping is the chipping occurs on certain and consistent positions of each cutting edge.

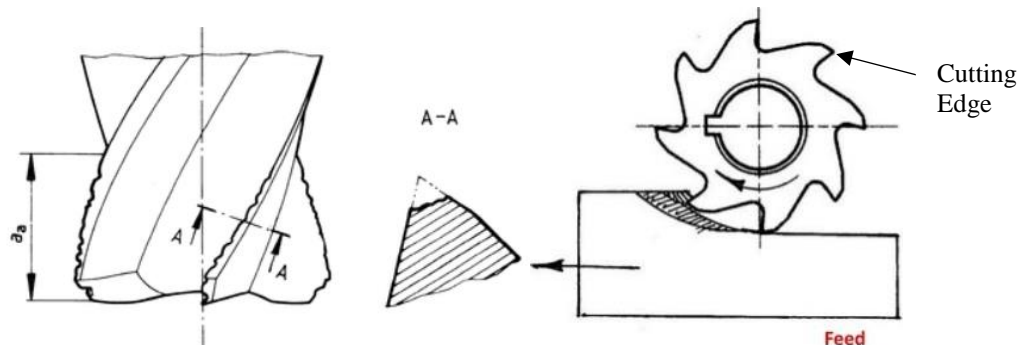


Fig. 1 The location of chipping on the milling tool [6]

2.2 Generation of chipping

The chipping has always been considered due to either excessive mechanical load or cyclic thermal load in the previous studies. The high mechanical load was investigated independently by the study [24], and the combination of the mechanical load and the thermal load was always considered as the mechanism of the chipping generation by most of the previous studies [25]–[28].

2.2.1 Mechanical load

The chipping along the boundary which caused by the mechanical fatigue cracks was found by Liu et al. [24]. The spindle speed used in the milling test was 10000 rpm and the feed rate was 0.1 mm per teeth. The chipping was found on the flank face of the milling tool.

2.2.2 Cyclic thermal load

Besides the mechanical load, the cyclic thermal load is another mechanism for the chipping generation under high cutting speeds to generate micro-cracks perpendicular to the cutting edge which is considered as the origin of the chipping [4]. This phenomenon has been well studied by Zhu's et al. [29] to describe the chipping formation as a debonding process with two steps. In the first step, since the thin layer of material from workpiece attaches on the cutting edge, the thermal conductivity of the cutting edge is decreased. As the increasing of the temperature on the cutting edge, the cracks along the longitudinal direction, which is shown in Fig. 2, were generated. In the second step, the partial cutting edge will be removed when these micro-cracks are too big to hold the cutting force. The similar research has been done by Jawaid et al. [30], and it has been realized that the thermal cracks started at some distance back from the cutting edge along the rack face and formed the chipping on the cutting edge.

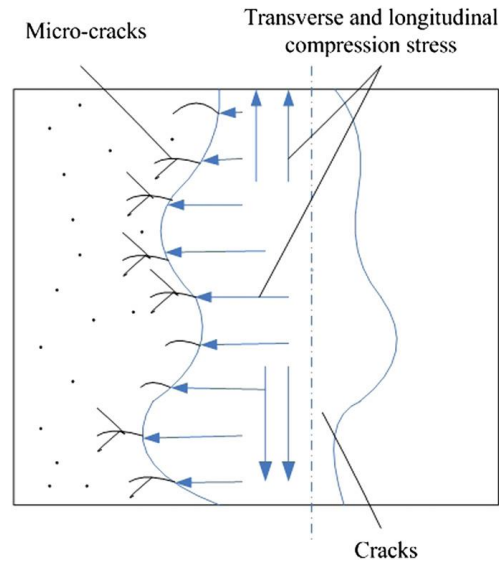


Fig. 2 The structure of the micro-cracks on the cutting edge [29]

Meanwhile, the cracks due to cyclic thermal loading can be significantly influenced by the flood coolant [31]. Nordin et al. [26] found that the cracks vertical to the cutting edge are mainly caused by the coolant. The vertical cracks were found in the milling experiment which was done under the cutting speed of 180 m/min and the feed rate of 0.24 mm per teeth. Firstly, the author assumed that the high temperature in the milling process will decrease the yield strength of the cutting edge which will have plastic deformation easily. Actually, the yield strength of the surface material on the cutting edge did not changed too much because of the coolant. Therefore, the plastic deformation of the inner material generated the compressive stress which caused the cracks vertical to the cutting edge named as comb cracks in Fig. 3.

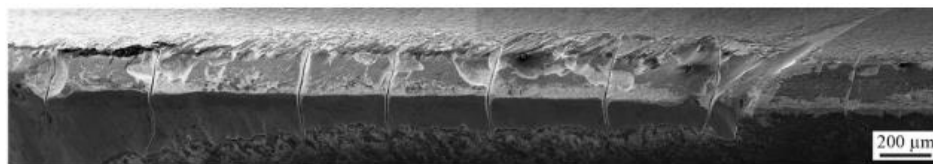


Fig. 3 Comb cracks [26]

2.2.3 Combination of high mechanical load and high thermal load

Mechanical load and cyclic thermal load always work together instead of working individually. Li et al. [27] found that the chipping in high-speed milling is mainly caused by the high cyclic thermal-mechanical impacts. The chipping was found on the PCD face milling tool when the cutting speed was higher than 250m/min. It is found that the width of chipping increases as the increasing of the cutting speed. Since the high cyclic thermal load and mechanical impact caused by the high milling speed, the cracks were generated and led to chipping at last.

Similar study was operated by Wolfe et al. [28], and it has found that both vertical and parallel cracks were observed on the cutting edge of PVD and CVD milling tools under the cutting speed of 213 m/min and the feed rate of 0.25 mm/tooth. In this study, the vertical cracks, which have shown in Fig. 4, were observed firstly, and parallel cracks between the vertical cracks were found after a period of time. Therefore, the significant chipping on the cutting edge was considered as the result of the interaction of the vertical cracks and the parallel cracks.

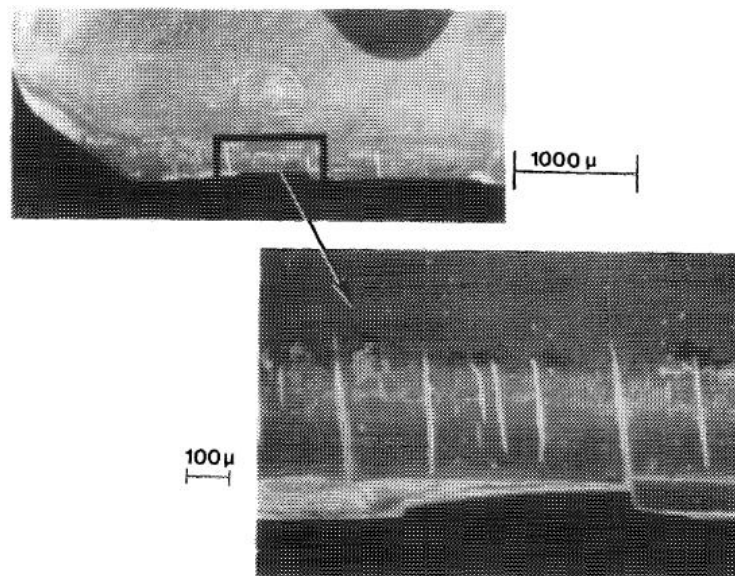


Fig. 4 The vertical cracks on the cutting edge [28]

The same mechanism of the chipping generation was also found by Nordin et al. [26]. It was found that the chipping was mainly caused by the propagation of the vertical cracks and the parallel cracks, and the chipping affected the tool life significantly.

2.3 Propagation of chipping

Santhanam et al. [31] observed that the chipping propagated with increasing of milling distance. The coated carbide milling tools were used to cut the 4140 steel, and the chipping was found as the determining factor to influence the tool life. The tool life of three milling tools with different coat is shown in Fig. 5. Both the width of uniform flank wear and the chipping were measured, but only the maximum number is shown as a set point in Fig. 5. Since the width of flank wear was only relative larger than the width of chipping at the beginning, this curve can be considered as the increasing of chipping. The author observed that the increase of the chipping followed by the number and severity of the thermal cracks. However, the slope of these three curves is not constant all the time. It is noticed that the slope at the end of the tool life is greater than the slope at the beginning for all the curves, but the author did not analyze this phenomenon.

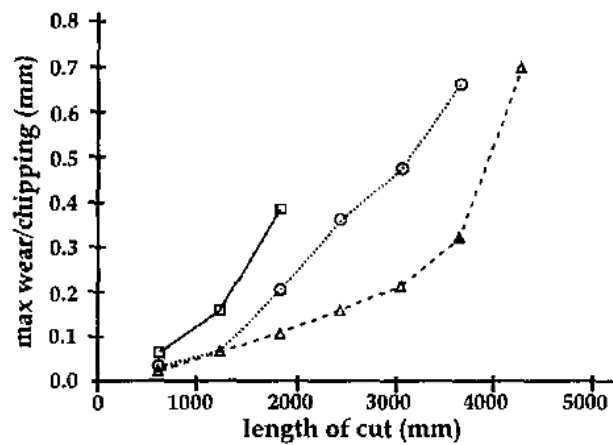


Fig. 5 Tendency of the maximum tool wear [31]

The different propagation rate of chipping under the high spindle speed was observed and analyzed by Chen and Li [11]. In this study, the coated tungsten carbide milling tools were used to cut the Inconel 718 under different cutting conditions. The width of chipping was measured after cutting the same length of material each time. The linear relationship with constant slope was observed between the propagation of the chipping and the cutting length at the spindle speed of 800 rpm and 1000 rpm. Since the high mechanical load was the only factor to influence the tool life under the 800 rpm and 1000 rpm, which are relatively low spindle speed, the relationship between the width of chipping and machined length was simple. However, the propagation with various speed was observed when the spindle speed was 1200 RPM. Since both mechanical load and the thermal load affect the chipping propagation under the spindle speed of 1200 rpm which is relatively high speed, the propagation rate of the chipping was not constant.

Except the high spindle speed, the geometry changing of the cutting edge was also considered as a reason for the various propagation rate of chipping. Li et al. [32] found that the cutting force will increase once the chipping occurred since the geometry of the cutting edge changed by the chipping. The increasing of the mechanical stress made the cutting environment worse which led to the propagation of the chipping. The similar conclusion has drawn by Jawaid et al. [33]. The author found that the compressive stresses on the cutting edge increased dramatically after the chipping occurred. Meanwhile, the compressive stress concentrated on the sharp part of the left cutting edge and generated the cracks. These cracks caused the propagation of chipping in the following milling process. However, the author did not analysis that why the chipping increased the cutting force which has been studied in the following research.

According to the study made by Saketi et al. [34], it is observed that the chipping led to the negative rake angle which increased the cutting force. However, the negative rake angle increased

the tool strength and decreased the tendency of the chipping propagation. Therefore, a balance between the geometry of the cutting edge and the chipping propagation may be existing and will be studied.

All the studies above were mainly focus on how the chipping itself propagate along the single cutting edge caused by the increased mechanical load and thermal load. However, the influence of increased mechanical load and thermal load on the other flutes of the same milling tool was not studied by the research above.

Su et al. [35] found that once the chipping occurs on one flute, the following flute will always cut the material under a higher chip load than the previous flute. The more detailed studied has done by Dae et al. [36]. The author found that the chipping will not only increase the cutting force of the flute where it occurs but also increase the cutting force of the following flute since the previously broken flute left an uncut area on the workpiece. This means that the next normal flute will remove more material than the normal situation. In other words, the chip load and cutting force of this normal flute will be increased. Theoretically, the chipping risk of this normal flute will be increased. However, the chipping propagation along different flutes was not observed in this study which could support the previous inference. Therefore, how the chipping influences and propagates along the other cutting edges with no chipping will be studied in this study.

2.4 Failure criteria

The chipping propagation has been studied extensively in the studies discussed in the previous section. When the chipping propagates to a certain width which is dependent on specific critical tolerances or requirements, the cutting tool is considered in the failure stage which is the end of the tool life and needs to be replaced. Even though the life of the same cutting tool can be different under specific conditions, the recommended tool life is still very meaningful for

comparative and analytic purposes. Typically, the chipping width is always combined with the flank wear width together as failure criteria to define the tool life. Regarding the milling operation, the similar failure criteria for cutting tools have been adopted by different previous studies as shown in Table 2.

Table 2. Combined failure criteria.

Reference	Failure criteria
ISO 8688-2:1989 [6]	Average uniform flank wear width = 0.012 in or Maximum localized flank wear width = 0.020 in or Chipping width = 0.020 in or Catastrophic fracture
Santos et al. [16]	Uniform flank wear width = 0.016 in or Crater wear depth = 0.004 in or Maximum localized flank wear width = 0.030 in or Chipping width = 0.030 in
Dewes et al. [37]	Maximum of flank wear width = 0.012 in or Chipping width = 0.012 in
Zhang et al. [7]	Average flank wear width = 0.3 mm or Maximum flank wear width = 0.6 mm or Chipping width = 0.5 mm
Santhanam et al.[31]	Uniform flank wear width = 0.4 mm or Localized flank wear = 0.75 mm or Chipping width = 0.75 mm

From Table 2, It has been noticed that different types of chipping were not distinguished in those criteria. Meanwhile, from the perspective of processing quality, the tool failure criterion is directly dependent on the shape changing of the cutting edge whatever the mode, chipping or

localized flank wear, to change the shape. Therefore, the critical chipping widths for those criteria have always been selected to be very closed to the critical widths of localized flank wear.

However, with the fixed numbers for the width of chipping used in the previous studies, which were only based on the quality requirement, it is hard to estimate when the width of chipping will meet the failure criterion. Since the chipping keeps extending in the milling process, it is highly probable that the tool life ends during the milling process. Consequently, the quality of the machined surface does not meet the requirement and the material has been wasted. Therefore, the milling tool should be replaced before start working if this tool is estimated to be a failed tool during the next milling process. The method to estimate the width of chipping will be studied.

Chapter 3 Research Gaps

It is known that the chipping is caused by the mechanical load and the cyclic thermal load that can be affected by varying the cutting conditions, such as spindle speed and chip load per tooth. The cutting conditions which caused the chipping were recorded by the previous study. However, there was no detailed analysis about the cutting conditions change the mechanical load and thermal load and generate the chipping consequently.

In the previous study, it is observed that the chipping not only influences the flute where it occurs, but also increases the cutting force hold by other flutes and the chipping risk of these flutes. However, the phenomenon that the chipping on one flute is caused by the chipping on other flutes has not been observed. It is hoped that this phenomenon can be observed in this study.

Once the chipping occurs, it will propagate in the following milling process. The different propagation rates have been observed, however, it was not analyzed in the previous studies.

Since the chipping decreases the geometric quality and surface quality of the machined part, the width of chipping was considered as a failure criterion of the milling tool. The failure criterial used in the previous study was recommended by ISO or decided based on the experience. However, it is hard to measure the width of chipping after each milling process. Therefore, a method to estimate the width of chipping is another gap of the previous research.

Typically, the tool life can be estimated by using the Taylor equation which is based on the tendency of flank wear extending. However, the relationship between the cutting distance and chipping propagation is not studied by the previous research. Therefore, the usability of Taylor equation when the chipping occurs and become dominate is unknown.

Chapter 4 Objectives

1. To identify the relationship between the chipping generation and the cutting conditions, e.g. spindle speed and chip load per tooth, during the end milling.
2. To analyze the impacts of chipping on a flute on the other flutes.
3. To investigate the mechanism of chipping propagation.
4. To verify if the Taylor equation can estimate the tool life accurately when the chipping is the dominating tool condition.

Chapter 5 Experimental Procedure

5.1 Cutting tool, equipment, and workpiece

5.1.1 Milling tool

Uncoated spiral four flutes solid carbide milling tools with the diameter of 1/4 inch were used in this study. Carbide milling tool can retain the cutting-edge hardness at the high machining temperature. The mechanical properties of the selected cutting tool are shown in Table 3.

Table 3. Mechanical properties of the milling tool.

Parameter	Value
Mill Diameter	1/4 in
Number of Flutes	4
Length of Cut	3/4 in
Shank Diameter	1/4 in
Overall Length	2- 1/2 in
Overhung Length	0.875 in
Helix Angle	30°

5.1.1 Workpiece

In this study, 1020 low carbon steel with the hardness of 86 HRB was selected as the workpiece material. The chemical composition and mechanical properties of 1020 steel have been elaborated in Appendix A and Appendix B. In order to maintain the constant cutting distance, the

material was cut 2 inches long.

5.1.2 Milling machine

All the experiments were conducted on a numerically controlled TRACK K3 EMX vertical milling machine, which is shown in Fig. 6, under dry, conventional end milling conditions. The available spindle speed of this machine tool ranges from 100 to 2500 RPM. Considering the primary purpose of this machine tool is prototyping and short run production of small-to-mid size complex parts, the limited rigidity of the machine can increase the tool vibration and further shorten the tool life, which can explain the reason why the actual tool life of milling tools in this study is always relative lower than it should be.



Fig. 6 TRACK K3 EMX vertical milling machine

5.2 Cutting conditions

The two independent variables used for the milling process are RPM and chip load per tooth. The variables being kept constant are workpiece material, milling tool, machine, axial depth of cut, and radial depth of cut. Also, the machine and operator were not changed during the whole experimental procedure in order to keep the consistency of the experiment.

5.2.1 Spindle speed (RPM)

The spindle speed (RPM) of the milling machine is defined as the rotation speed of the spindle and measured in revolutions per minute. The cutting speed, which is the primary factor to influence the cutting process by varying the deformation rate of the workpiece material being cut and the heat generated by friction, can be calculated by multiplying the RPM by the perimeter of the cutting tool. Therefore, RPM has been selected to be one of the variables to be controlled in this study. Based on the availability of the milling machine used in the experiments, spindle speeds were selected from 100 RPM to 2500 RPM.

5.2.2 Chip load per tooth (CLPT)

As the other important cutting parameter to be controlled by this study, the Chip load per tooth (CLPT) is the amount of material removed by each flute of milling tool in each rotation and measured in inch. In the milling process, the metal removal rate and surface finish can be directly affected by the CLPT. In addition, the CLPT is also related to the cutting force and the cutting temperature.

Considering the actual rigidity and the power of the milling machine used by this study and the preliminary study, the cutting tools can be held firmly by using half of the recommended values from 0.0008 in to 0.003 in, which are also the available chip loads selected in this study. Unlike

the turning process, the chip load is not a machining parameter to be controlled directly in the milling process and can be estimated by the combination of the spindle speed, the number of cutting flutes, and the feed rate according to the following equation.

$$Feed\ Rate = CLPT \times RPM \times Number\ of\ Flutes \quad (2)$$

5.2.3 Axial depth of the cut & radial depth of cut

Besides the spindle speed and the chip load, the axial depth of cut (ADOC) and the radial depth of cut (RDOC) are two other machining parameters in milling which needed to be selected in this study. ADOC is the distance between the bottom of the milling tool and the uncut surface of the workpiece. Considering the tool wear is uniformly distributed along the cutting edge, the ADOC is not considered as a variable in this study, and the fixed value 0.12 in which is recommended by the handbook has been selected for all the experiments.

The radial depth of cut (RDOC) is the distance a milling tool is stepping over into the workpiece. As shown in Fig. 7, by varying the RDOC, the cutting distance and uncut chip thickness are changed accordingly. However, these two effects generated by the variable RDOC can also be studied by changing the spindle speed and the chip load as described before. Thus, RDOC is also selected as a constant value (0.09 in) for all the cutting experiments in this study.

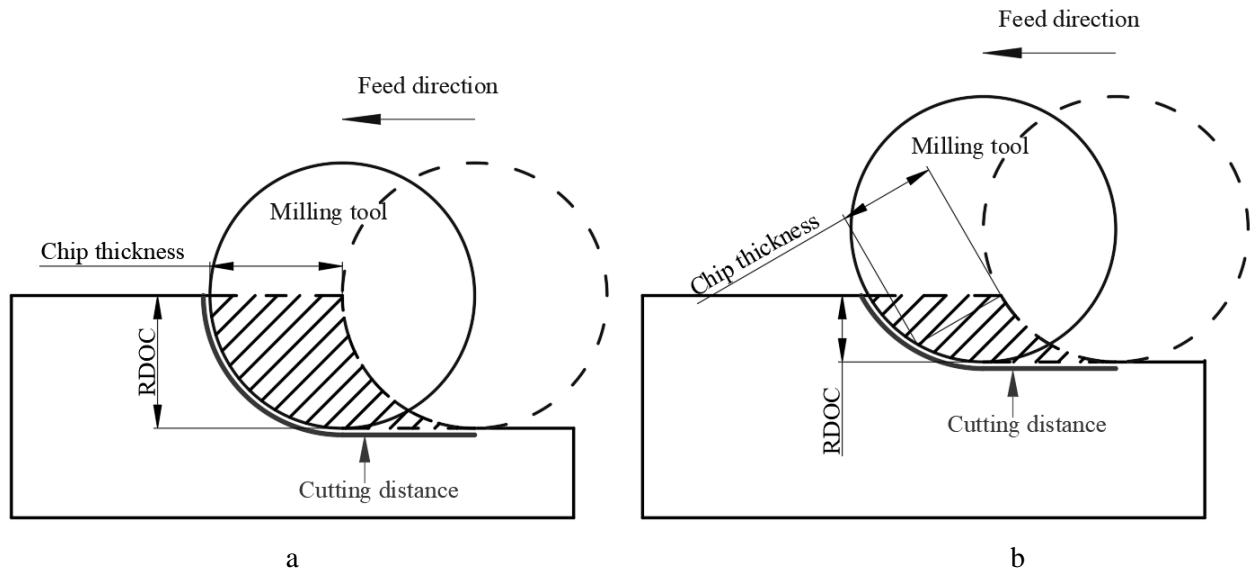


Fig. 7 (a) High RDOC (b) low RDOC

Based on the cutting conditions listed above, all the combinations of the cutting conditions used in the experiment are listed in Appendix C.

5.2.4 Milling process

The milling process used in this study is conventional dry milling. Comparing the conventional milling with climb milling, the chip thickness starts from the maximum value and decrease to zero when using the climb milling. Therefore, the climb milling generates more mechanical shock than conventional milling. Considering the rigidity of the milling machine, the conventional milling process was used in the experiments.

In addition, the coolant was not used in the experiments. Because the method to deliver the coolant, which includes the properties and pressure, is a variable which is hard to control.

5.3 Observation equipment

5.3.1 Digital microscope

To improve the efficiency for tool wear check, a KLAREN USB Digital Microscope, which is shown in Fig. 8, was used to operate the preliminary check for different tool wear modes, including flank wear, crater wear, chipping, and BUE appeared. All the observations were qualitatively recorded, and more accurate measurements were obtained by the following measurements using the profilometer.



Fig. 8 KLAREN USB Digital Microscope

5.3.2 Surface Profilometer

In this study, a WYKO NT1100 dynamic profilometer, which is shown in Fig. 9, was used to observe wear land on the flank face. The WYKO NT1100 is an optical profilometer which uses the reflected light from the detecting surface to observe and measure wear land on the surface. In general, the wear land on the flank face and flank face itself are not on the same plane, and the

surface can only be observed when it is perpendicular to the emitted light from the profilometer. Therefore, as shown in Fig. 10, the flank face and wear land cannot reflect the light to the profilometer together, which means they cannot be observed at the same time. Due to the mechanism mentioned above, the wear land can be distinguished from the flank face and be measured by WYKO NT1100 dynamic profilometer.



Fig. 9 WYKO NT1100 dynamic profilometer

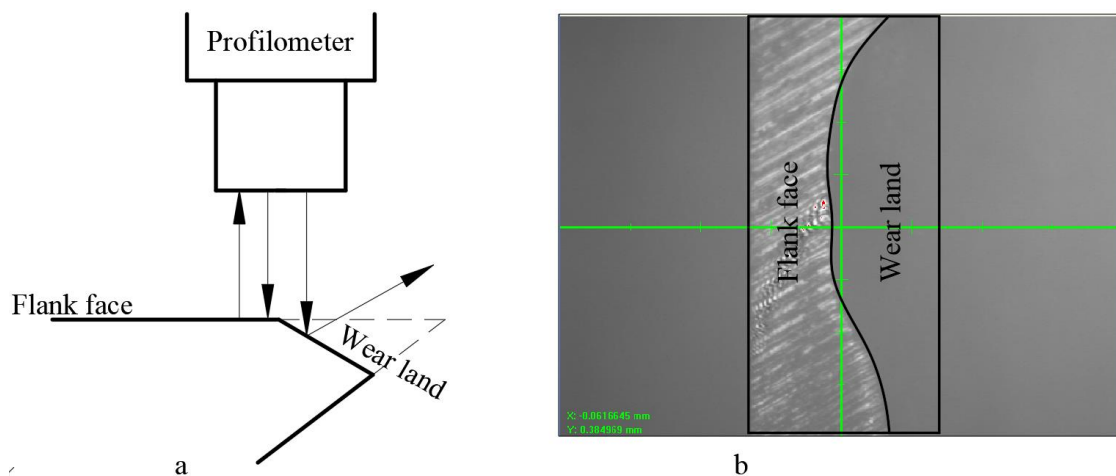


Fig. 10 (a) Flank face is reflecting the light to profilometer (b) Wear land is reflecting the light to the profilometer

However, the generation of wear land was caused by either the flank wear, chipping, or both. Therefore, it is necessary to distinguish the flank wear and chipping to study them separately. The method used in this study is based on the image of the wear land. The wear land image of flank wear is a whole bright strip. However, some parts of the chipping wear land are dark in the image. This phenomenon will be explained below.

It is known that the flank wear is caused by the friction between the machined surface and the flank face, and the material of the cutting edge is removed gradually. Therefore, the wear land of flank wear is a flat surface which can reflect the light when it is facing to profilometer. It means that the whole image of the wear land can be observed when the orientation is property. However, it is hard to obtain the image of the whole chipping wear land.

The chipping is jagged along the cutting edge, which is shown in Fig. 11 (a), when the flank face of the milling tool is facing the profilometer. However, the actual chipping wear land, which is shown in Fig. 11 (b), is not a flat surface. Therefore, the chipping wear land cannot reflect all the light to the profilometer when it is vertical to the light. In other words, the image of whole chipping wear land cannot be obtained since part of the chipping wear land is dark under the profilometer.

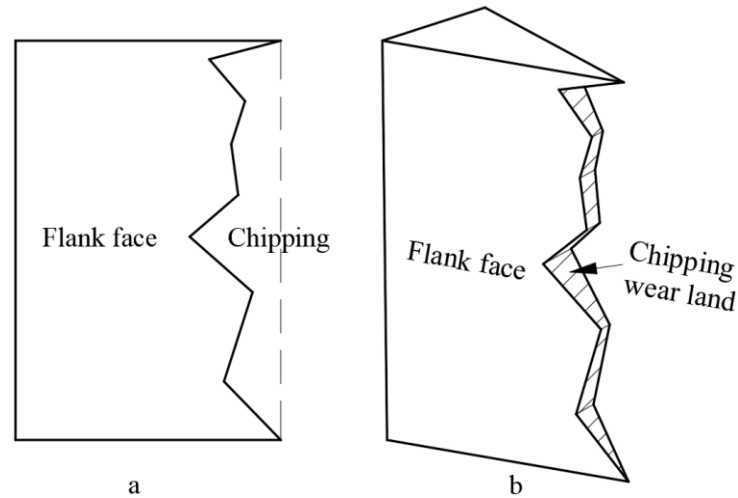


Fig. 11 (a) Shape of chipping when the flank face is vertical to the light (b) actual chipping wear land

5.4 Procedure

The experimental procedure has two stages which are the initial stage and the follow-up stages. All the suitable cutting conditions were identified in the initial stage, which has also been used for the experiments in the follow-up stages. In the follow-up stages, a repeatable processual was repeated until the width of chipping on every milling tool meet the failure criterion which will be explained in the following section.

5.4.1 Initial stage

All the available cutting conditions were found out in the initial stage by following the chart which is shown in Fig. 12.

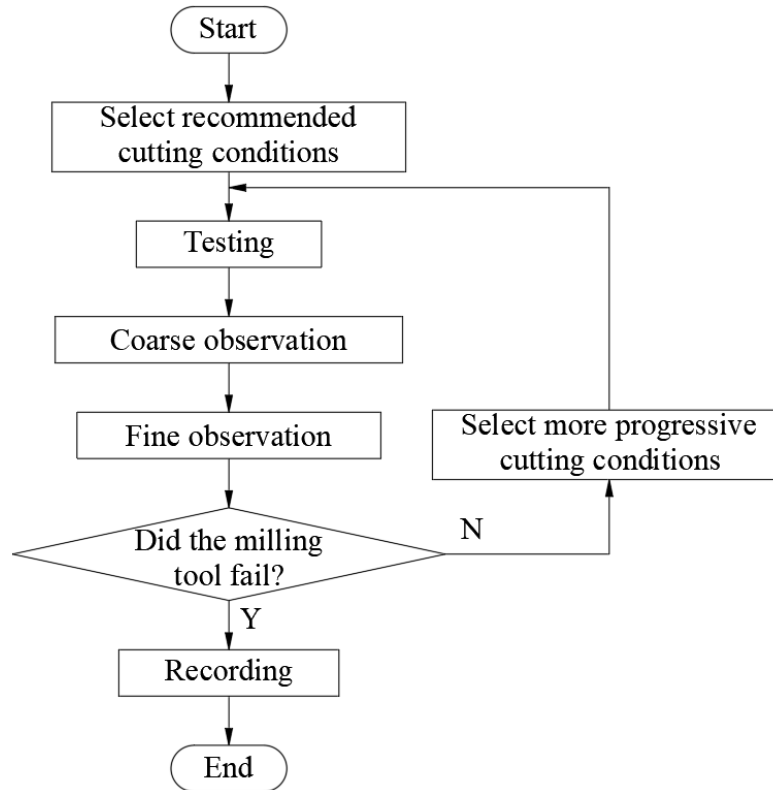


Fig. 12 Procedure of the pretest

The cutting conditions used in the first loop of the initial stage were the recommended cutting conditions from the handbook. Some new milling tools were used to cut 2 inches of the workpiece under the selected cutting conditions.

After the milling process, the type of tool conditions and the availability of the milling tool was checked by the digital microscope. In order to check the usability for used tools, the cutting zone, which are the colored parts in Fig. 13 (a) and Fig.13 (b), was used as a criterion to stop the milling process. Since the damage in Fig. 13 (a) is within the cutting zone, this tool was considered as usable. However, the tool in Fig. 13 (b) should not be used to mill the workpiece because part of the tool damage has exceeded the cutting zone.

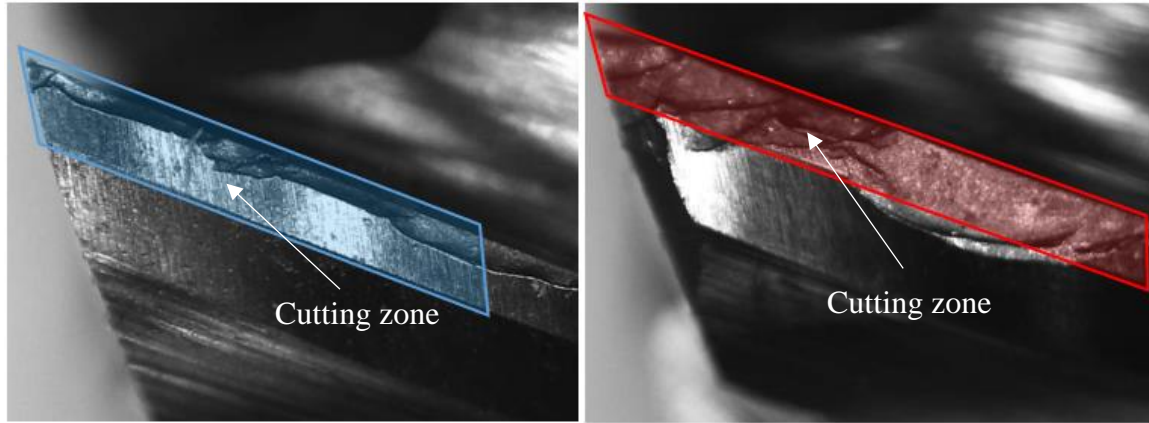


Fig. 13 (a) usable milling tool (b) unusable milling tool

Except the obvious failure tool conditions found by the digital microscope, other tool conditions were measured in the fine measurement step. The WYKO NT1100 Dynamic Profilometer was used to measure the width of flank wear and the width of chipping.

The width of flank wear is the distance from the original cutting edge to the end of the flank wear. However, the width of flank wear in this study was too small, and the flank wear did not change the cutting edge significantly. Therefore, the width of flank wear in this study is the distance from the existing cutting edge to the end of the flank wear. The width of chipping is the distance from the original cutting edge to the end of the chipping[6]. However, the original cutting edge cannot be observed if the chipping appears. Therefore, the distance from the end of the chipping to the end of the cutting zone and the width of the cutting zone were measured, and this part was called the remaining part in this study. The width of chipping is equal to the difference between the width of the cutting zone and the width of the remaining part. The width of flank wear and width of chipping is shown in Fig. 14.

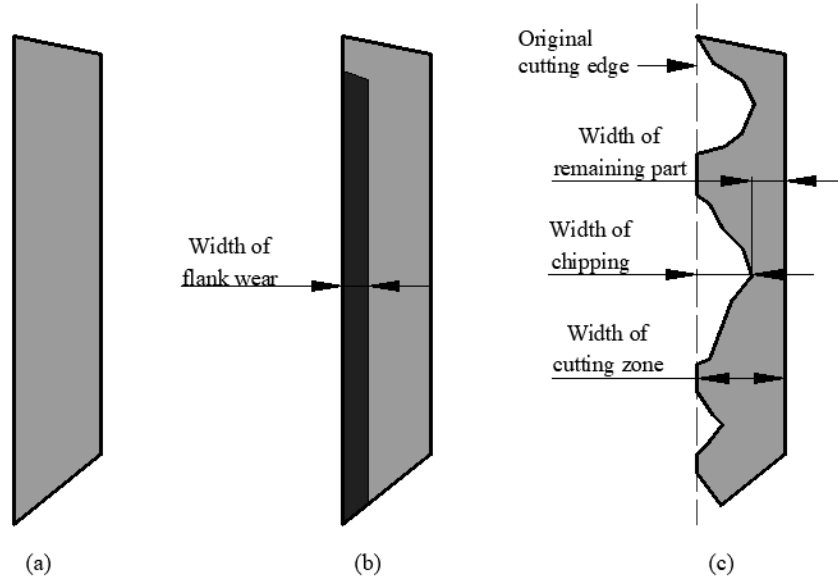


Fig. 14 (a) The new cutting zone (b) The cutting zone with flank wear, and the dark blue part is the flank wear (c) The cutting zone with chipping, and the parameters were used to calculate the width of chipping

The width of widest flank wear and the widest chipping were recorded as the “maximum flank wear” and “maximum chipping” in the map. Also, the average of all the width of flank wear and the average of all the chipping in the cutting zone were calculated and recorded as “average flank wear” and “average chipping.” The method of calculating the average flank wear and average chipping is shown in Equation 2 and Equation 3.

$$\text{Average flank wear} = \frac{\text{Sum of all the width of flank wear}}{\text{Number of flank wear}} \quad (3)$$

$$\text{Average chipping} = \frac{\text{Sum of all the width of chipping}}{\text{Number of chipping}} \quad (4)$$

The parameters of the tool conditions were compared with the failure criteria in order to decide if the cutting conditions were useable or too progressive. If the tool conditions did not meet the failure criteria, this means the corresponding cutting condition is useable for the standard

experiment. Therefore, more progressive cutting conditions, which have not been covered before, were selected. The more progressive cutting conditions include higher RPM, lower RPM, higher CLPT, and lower CLPT.

The new milling tools were used to cut another 2 in of the workpiece under the selected cutting conditions. The coarse observation and the fine observation were done after the cutting process and the result is shown in Appendix E. The tool conditions were compared with the failure criteria, and the cutting conditions for the following cutting test were decided based on the result of the comparison. All the procedures were repeated until all the useable cutting conditions were tested.

Five cutting conditions in the Fig. 15 can be taken as the instances to explain the process of initial stage. Firstly, the RPM of 300, 800 and 1200 have been used under the CLPT of 0.003 in, and these cutting conditions were considered as useable cutting conditions after the measurement. Therefore, the RPM of 1400, which is higher than 1200, and the RPM of 100, which is lower than 300, were tested under the same CLPT. Since both of two cutting conditions caused the tool failure, the RPM higher than 1200 or lower than 300 under the CLPT of 0.003 were considered as the progressive cutting conditions and were not used in the follow-up stage. The same method was also been used to find the useable cutting conditions under the constant RPM. By repeating this process, the map in the Fig. 15 was obtained which shows the boundary between the useable cutting conditions and the progressive cutting conditions. In other words, all the useable cutting conditions were used in the follow-up stage were found.

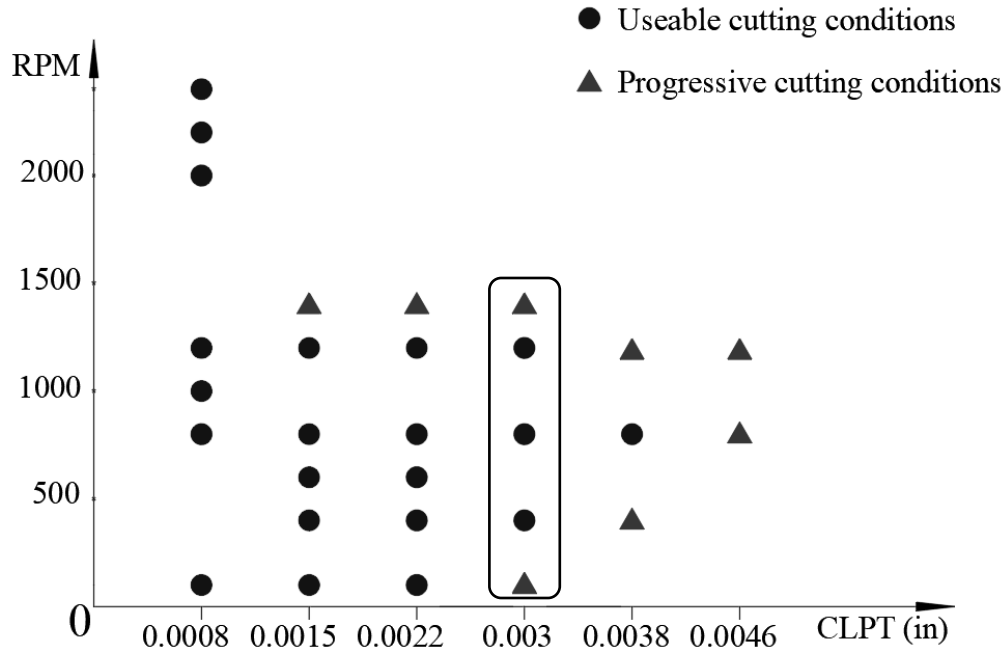


Fig. 15 Map obtained from initial stage

5.4.1 Follow-up stage

In order to measure the tool life over a wide range of cutting conditions, e.g., the spindle speed and the chip load), the brand-new milling tool has been used for each combination of those two machining parameters. In this study, the cutting length, instead of the actual cutting time, has been selected to specify the tool life. To trace the tool life systematically, all the cutting tools were checked and measured after the same cutting length, e.g., 2 inches in this study, which will be considered as one stage, and this procedure will be repeated until all the tools are failed. The steps of one loop are shown as the flow chart in Fig. 16.

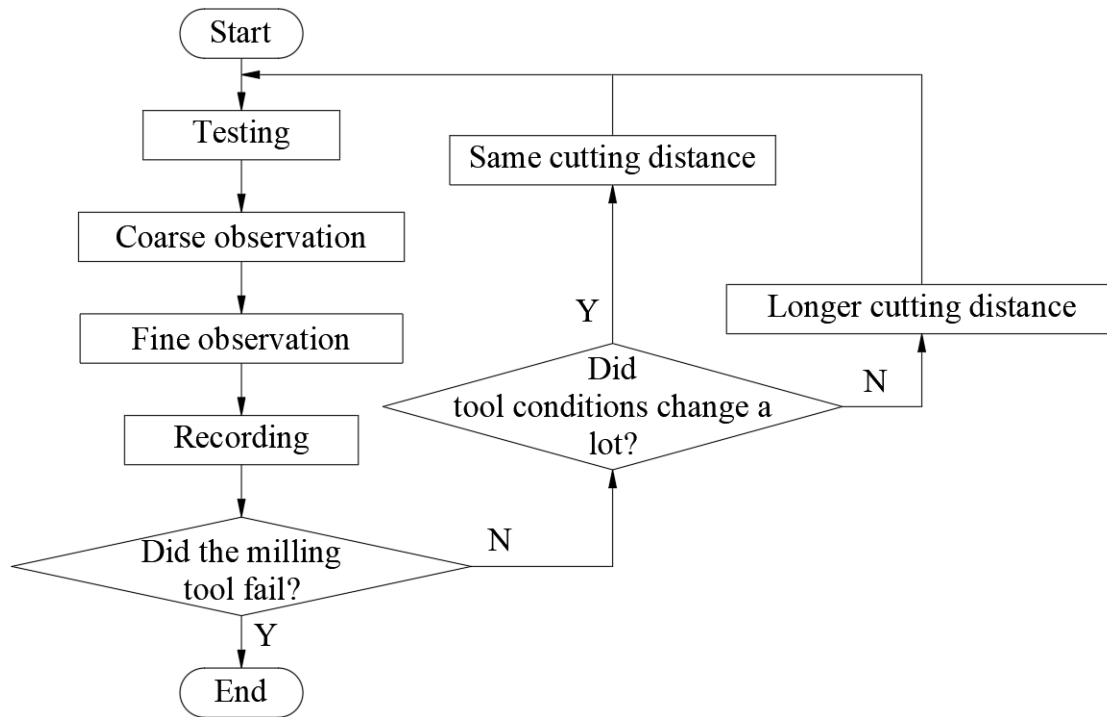


Fig. 16 Follow-up stage

At the beginning of the follow-up stage, the cutting distance was only 2 in. The coarse observation and the fine observation were the same as what has been done in the initial stage.

In the following step of recording, the tool conditions were recorded on a map, and the tool condition included the type of tool conditions, the average width of chipping, the maximum width of chipping, the average width of flank wear, and the maximum width of flank wear. One of the maps is shown in the Appendix G. In this map, the X-axis and Y-axis are the CLPT and RPM respectively. Every used cutting condition is represented by a circular mark. The blue circles stand for the milling tool which is still available after cutting a specific distance of the workpiece. In addition, the cutting conditions are listed with each data point on the map. The red triangle means the milling tool is failed after cutting a specific distance of the workpiece under the cutting condition what this triangle represents on this map. If the tools are still available, they would be used the constant cutting conditions in the next loop.

Before starting the next loop, the parameter of the tool conditions was compared with the tool conditions on the same milling tool in the previous loop. The next loop was started at the selecting cutting conditions after the drawing map of this loop. If the variation of the tool conditions were not greater than 5% of the width of cutting zone in several continuous test, the cutting distance of the next test was increased. Otherwise, the cutting distance was kept constant. The tool conditions of each tool from the first loop to the sixteenth loop are shown form Appendix F-1 to F-16. The cutting distance used in each loop was included in the map of each loop and shown in Appendix D. In the following loops, all the previous steps were repeated until all the milling tools failed.

Chapter 6 Results & Discussion

In this chapter, the chipping formation and development will be investigated with the following sequence: the chipping behaviors in different tool locations (Section 6.1), the effect of cutting conditions on chipping (Section 6.2), and the interaction among different flutes (Section 6.3), the mutual effect between the tool wear and chipping (Section 6.4), the chipping progression in terms of cutting distance (Section 6.5), and the usability of Taylor equation (Section 6.6).

6.1 Chipping behaviors in different tool locations

Typically, the cutting zone on each flute of the cutting tool can be classified into three regions as shown in Fig. 17, which are the corner region, the edge region, and the depth-of-cut region. Considering the complex geometry of the cutting tool, different locations of the same cutting tool experience quite different cutting conditions during the cut, which can further lead to various processes in chipping development.

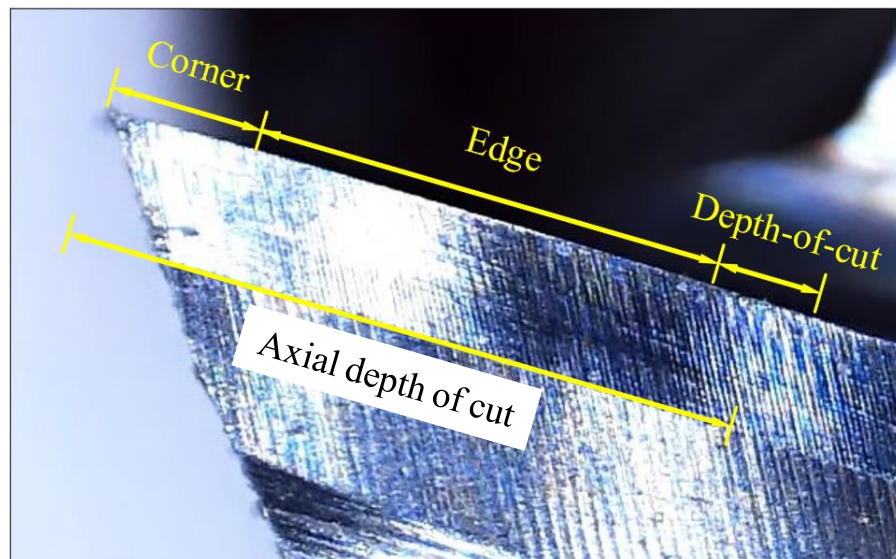


Fig. 17 Three cutting region of the cutting edge

The corner of the flute is the first region of contact in cutting to take the impact load. The less tool material in this region largely reduces the toughness of the corner to produce the breakage, especially under the vibratory cutting process. Due to nature of the milling operation, the successive contacts can generate impact loads to damage sharp corners of cutting tool flutes within a short cutting distance, which has been observed in most of the cutting experiments. Especially as shown in Fig. 18, the corner breakage became more obvious under high chip loads which can generate higher impact loads (Tools #4).

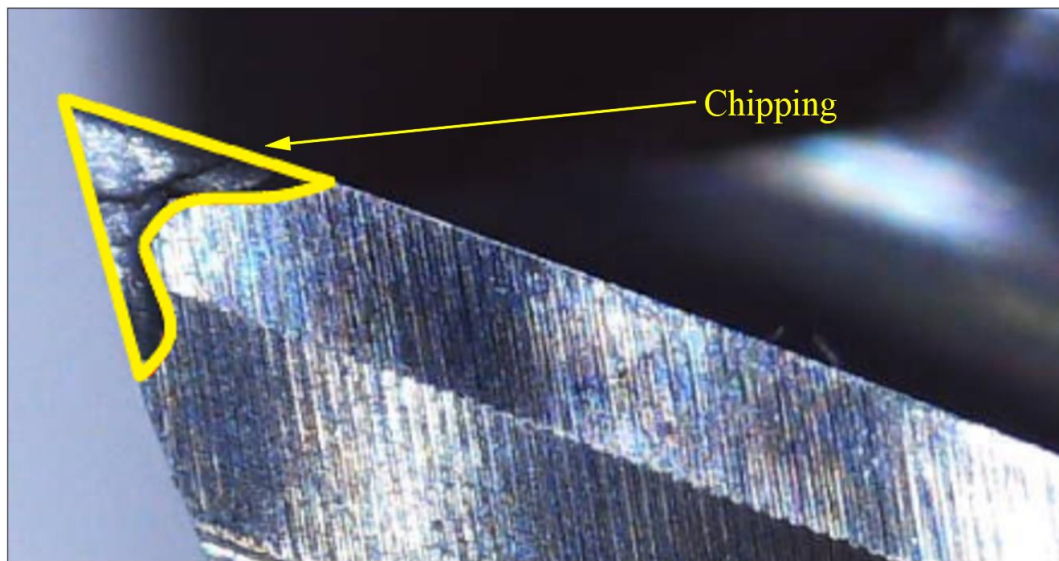


Fig. 18 The chipping in the corner region of the tool #4

The edge region is the main part of the cutting tool flutes to cut the material. Similar to the corner breakage, the edge chipping always appears on the sharp cutting edge due to the reason that the limited tool material on the edge is not strong enough to take the loads or vibrations and chipped off from the tool to form the chipping. Even though the chipping always results in high cutting force and rough cutting surface, the cutting tool could also benefit from the chipped edges to have more material to take the cutting loads for a longer cutting distance, which will be further discussed

in the section 6.5. However, the mild chipping can be considered as a self-adjustment of the cutting tool to accommodate to the harsh cutting conditions, and the dull cutting edge can help to prevent chipping and extend the tool life for rough cutting.

The depth-of-cut region is located at the end of the cutting depth, where is the boundary between the parts of edge in cutting and out of cutting. In this study, the constant depth of cut has been set up to 0.12 inch. The quite different loading conditions in two parts around the depth of cut region to initiate the chipping and cause the chipping to develop in a rapid and severe manner. Based on experimental observations of this study as shown in Fig. 19, most of the chippings appeared first in this region and developed into severe breakages finally to fail cutting tools. This type of chipping can be reduced by varying the depth of cut in different operations or increase the helix angle to enlarge the contact area between the cutting tool and the workpiece material.

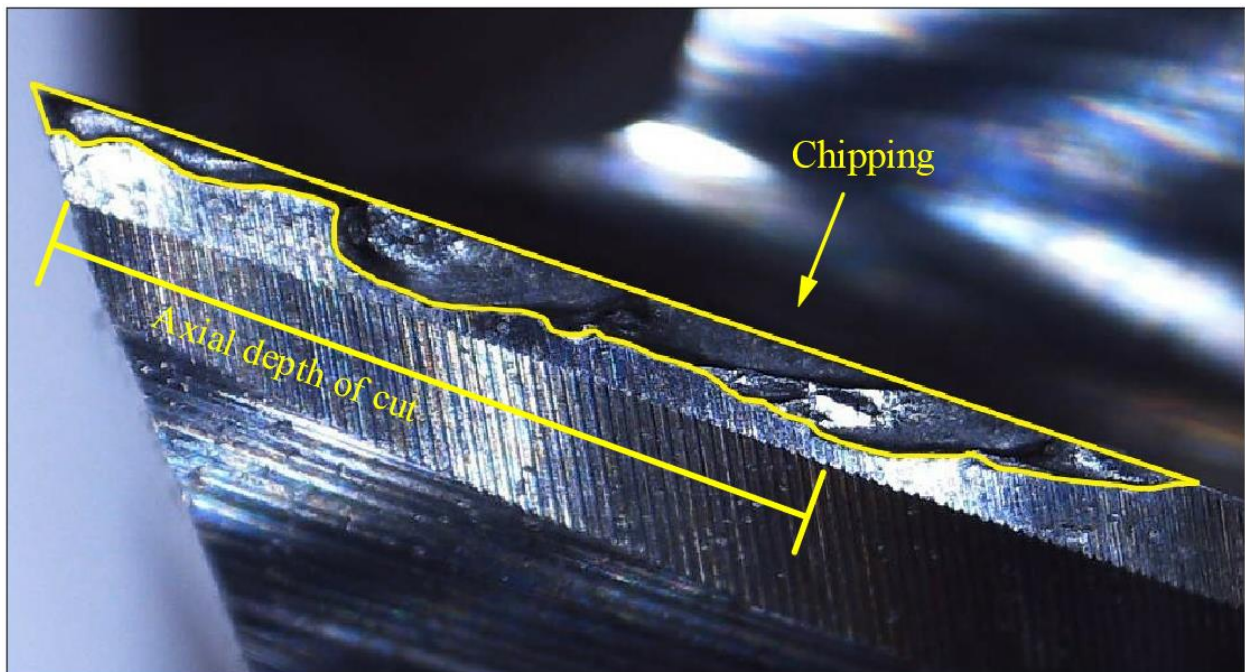


Fig. 19 The chipping located on the depth-of-cut region

6.2 Effects of cutting conditions on chipping

To investigate the effect of cutting conditions on chip formation, cutting tests have been operated under a wide range of cutting conditions, i.e. RPM and chip load, over a short and constant cutting distance of 2 inches. After each cut, all the cutting edges were inspected for different types of tool conditions which also were measured. The usable cutting tools will be used for more 2-inch cuts until the failure.

Typically, the cutting tool chipping is mainly caused by the mechanical loading, the thermal cycling, or both of them [30]. Considering the highest RPM used in this experiment was not high enough to generate high temperatures, the chipping due to thermal cycling will not be considered in this study, which agrees with the fact that no clear microcracks perpendicular to the cutting edge have been captured by the experimental observations. Therefore, in this study the chipping mechanism will be investigated and explained mainly based on mechanical loadings applied on cutting tools.

6.2.1 High RPM and low chip load

It is found that the RPM of tool #24 and tool #31, which cut the longest distance of workpiece, were highest which were 2200 and 2400, and the chip load was lowest which was 0.0008 in. Under the high RPM and low chip load, the high cutting force is mainly caused by the low chip load.

In end milling, the rake angle is positive when the chip load is reasonable as shown in Fig. 20 (a). However, the rake angle is negative when the chip load is extremely low as shown in Fig. 20 (b) since the tip of cutting edge cannot be perfect sharp. The decreasing of the rake angle leads to the increasing of the cutting force. Meanwhile, the high RPM increased the temperature of the

material in the contacting area, and the thermal softening happened. However, since the RPM was high enough, the thermal softening was not found to be dominate and did not decrease too much of the cutting force. Therefore, the cutting edge could not hold the cutting force under the high RPM and low chip load without the chipping.

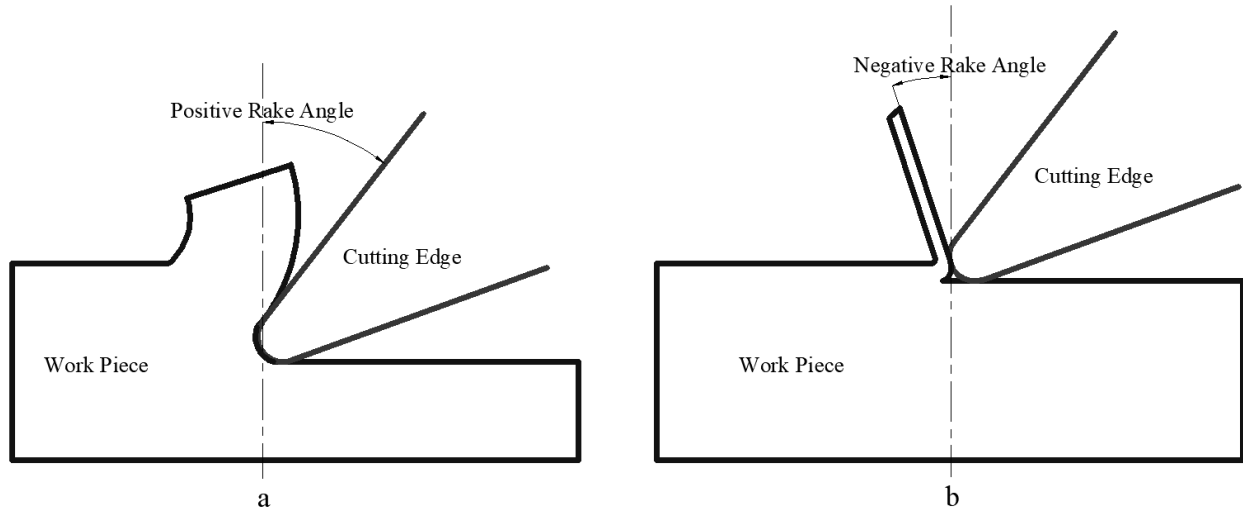


Fig. 20 (a) The rake angle is positive when the chip load is reasonable (b) The rake angle is negative when the chip load is low

6.2.2 Low RPM and low chip load

The cutting force under the low RPM and low chip load is higher than the cutting force under the high RPM and low chip load. In order to hold the cutting force, the milling tool which used low RPM and low chip load lost more material of the cutting edge after cutting the same distance of workpiece.

The comparison of tool #2 and tool #31 can be taken as an instance. The RPM of tool #2 and the tool #31 were 800 and 2400. The chip load of the tool #2 and the tool #31 was 0.0008 in. Since the RPM of tool #31 is higher than the tool #2, more thermal generated by the tool #31 and

reduced more cutting force than tool #2. Therefore, the width of chipping on the tool #31 was smaller than the chipping on the tool #2 after cutting 8 inches of workpiece. The chipping on the tool #31 and the chipping on the tool #2 after cutting 8 inches of workpiece are shown in the Fig. 21 (a) and Fig. 21 (b).

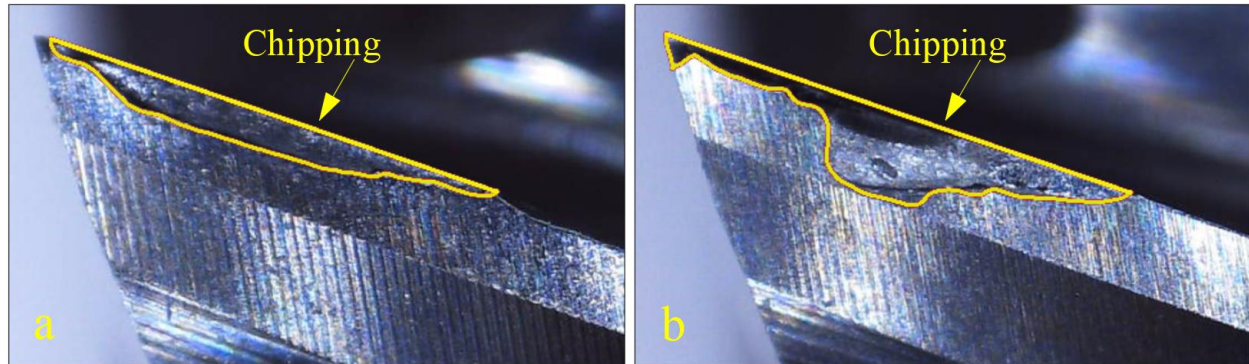


Fig. 21 (a) the chipping on the tool #31 after cutting 8 inches of workpiece (b) the chipping on the tool #2 after cutting 8 inches of workpiece.

6.2.3 Low RPM and high chip load

When the RPM and cutting distance were same, it is found that the chipping on the milling tool was wider when using the higher chip load than using the lower chip load. Due to the strain hardening, the cutting force increased when using the higher chip load. In order to hold the high cutting force, more material was removed from the cutting edge. Therefore, the chipping was wider when using the higher chip load.

The comparison of tool #2 and tool #29 can be taken as an instance. The RPM of tool #2 and the tool #29 was 800. The chip load of the tool #2 and the tool #29 were 0.0008 in and 0.0046 in. Since the chip load of tool #29 is higher than the tool #2, the hardness of the material at contacting area was higher when tool #29 doing the cutting work. Therefore, the width of chipping

on the tool #29 was larger than the chipping on the tool #2 after cutting 2 inches of workpiece. The chipping on the tool #2 and the chipping on the tool #29 after cutting 2 inches of workpiece are shown in the Fig. 22 (a) and Fig. 22 (b).

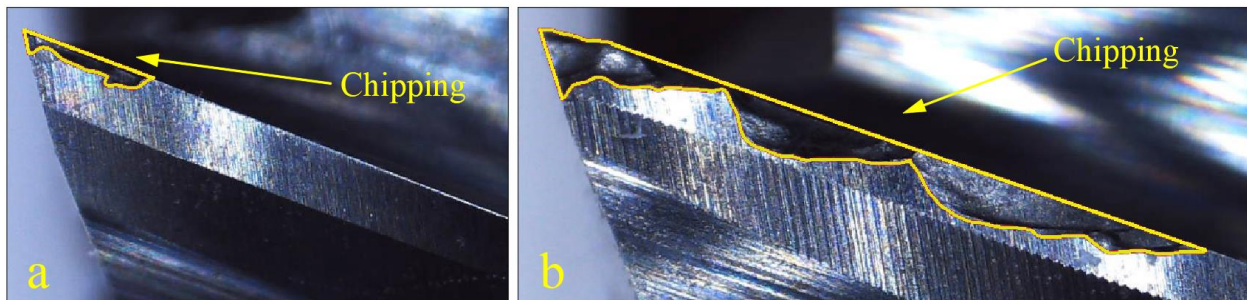


Fig. 22 (a) the chipping on the tool #2 after cutting 2 inches of workpiece (b) the chipping on the tool #29 after cutting 2 inches of workpiece.

Based on the observations, most of cutting tools failed eventually due to the severe chipping with different developing processes. Under extreme cutting conditions, such as the high cutting speed or the high chip load, several cutting tools, i.e. tool #1, tool #29 and tool #32, failed immediately due to the large chipping within the first two-inch cut, and the development of the entire process is too quick to be observed. In addition, the chipping developed with a

In the milling process, most of the milling tools reached the ending point of experiment after cutting a short distance of workpiece which is less than 10 inches. Only two milling tools cut a long distance of workpiece which include tool # 24 and tool # 31. It is found that the chipping is a way that the cutting edge uses to change the geometry of itself to hold the cutting force. The different width of chipping on the cutting depends on the cutting force under different cutting conditions. The extension of chipping and the how the cutting conditions affect the chipping will be discussed in this section.

6.3 Chipping propagation among different flutes

Chipping is considered as one type of tool wear that results in sudden loss of cutting tool material. Due to the suddenness of this generation process, the chipping sometimes appears on individual flute of the cut tool first and cutting capability of the flute will be reduced to leave more material and rough cutting surface to the next flute. Therefore, the chipping is always can be observed to propagate from one flute to the next one with the similar pattern and location.

Based on our experimental observations, the chipping development of the tool #12 can be used as an instance to investigate the chipping propagation among different flutes. As shown in Fig. 23 (a) and (b), the chipping has only been observed on the fourth and first flute with a cutting length of 2 inches. The second and third flute were good as shown in Fig. 23 (c) and (d).

After finishing another 2 inches, the chipping has been developed in the fourth and first flute which has the chipping before as seen in Fig. 23 (e) and (f), the very similar chipping pattern has also been observed on the following second flute, as shown in Fig. 23 (g), which has no chipping previously. The Fig. 23 (h) is the third flute.

After cutting 6 inches totally, the chipping on the fourth and first flute did not extend too much as shown in Fig. 23 (i) and (j). However, the chipping on the third flute became bigger which is shown in Fig. 23 (k). Meanwhile, the new chipping appeared on the third flute which did not have any chipping previously as shown in Fig. 23 (l).

From the chronological order and the location of the appearance of the chipping in different flutes, it can be concluded that the chipping can be propagate among different flutes following the cutting sequence, due to the rough surface and the higher chip load left from the previous chipped flute to the following ones. In addition, the entire process of chipping propagation among different flutes always happen within a very short period, which is very hard to be identified for most of

observations in this study.

Considering the fact that the chipping on individual flute can easily influence and propagate to other flutes of the same tool to generate the similar chipping condition, it is good enough to use the maximum chipping width among different flutes, instead of the average value, to determine the cutting tool condition comparing with the failure criterion for chipping, which has also been adopted by this study.

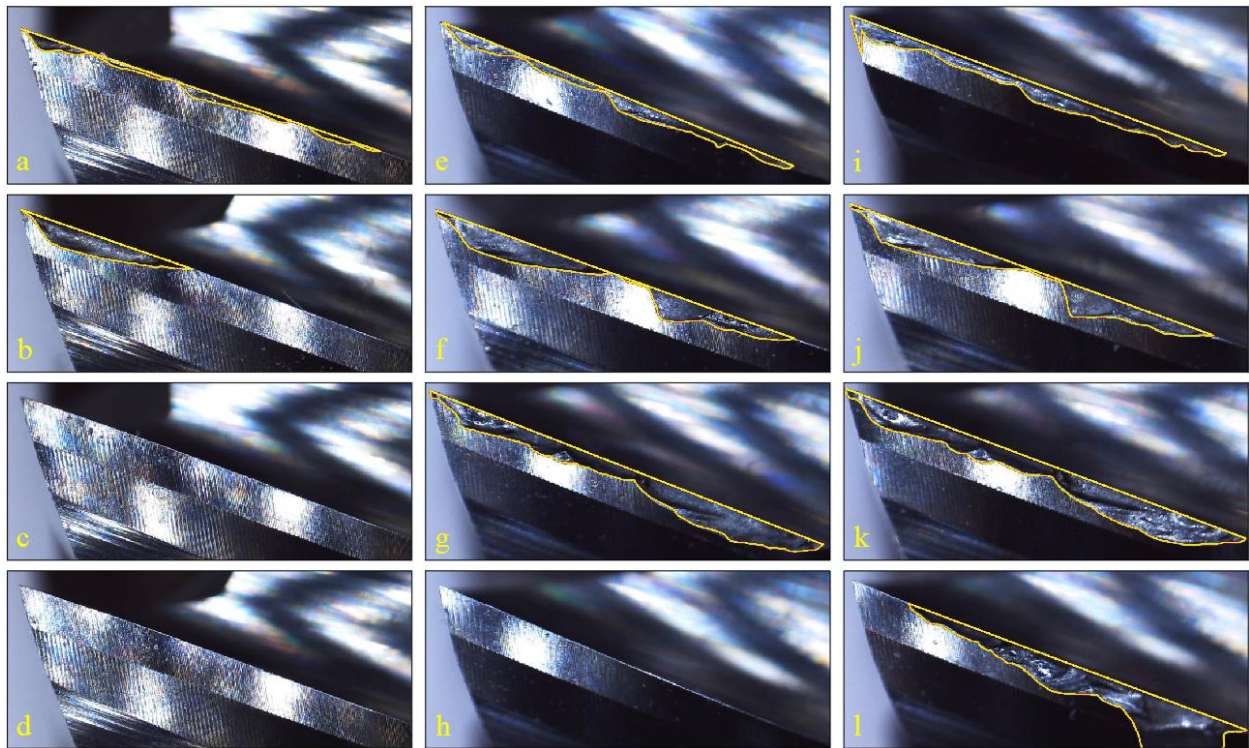


Fig. 23 (a) the fourth flute after cutting 2 inches (b) the first flute after cutting 2 inches (c) the second flute after cutting 2 inches (d) the third flute after cutting 2 inches (e) the fourth flute after cutting 4 inches (f) the first flute after cutting 4 inches (g) the second flute after cutting 4 inches (h) the third flute after cutting 4 inches (i) the fourth flute after cutting 6 inches (j) the first flute after cutting 6 inches (k) the second flute after cutting 6 inches (l) the third flute after cutting 6 inches

6.4 Chipping progression in terms of cutting distance

6.4.1 The extension of the chipping in long cutting distance

During cutting the long distance of workpiece, the variation of chipping was found to be constant sometimes instead of keep extending during the experiment. Since all the chipping on these milling tools stopped extending at some period, one of the chipping on each milling tool, which appeared before the chipping kept instance, were selected and observed. The variation of the width of these chipping is shown in Fig. 24.

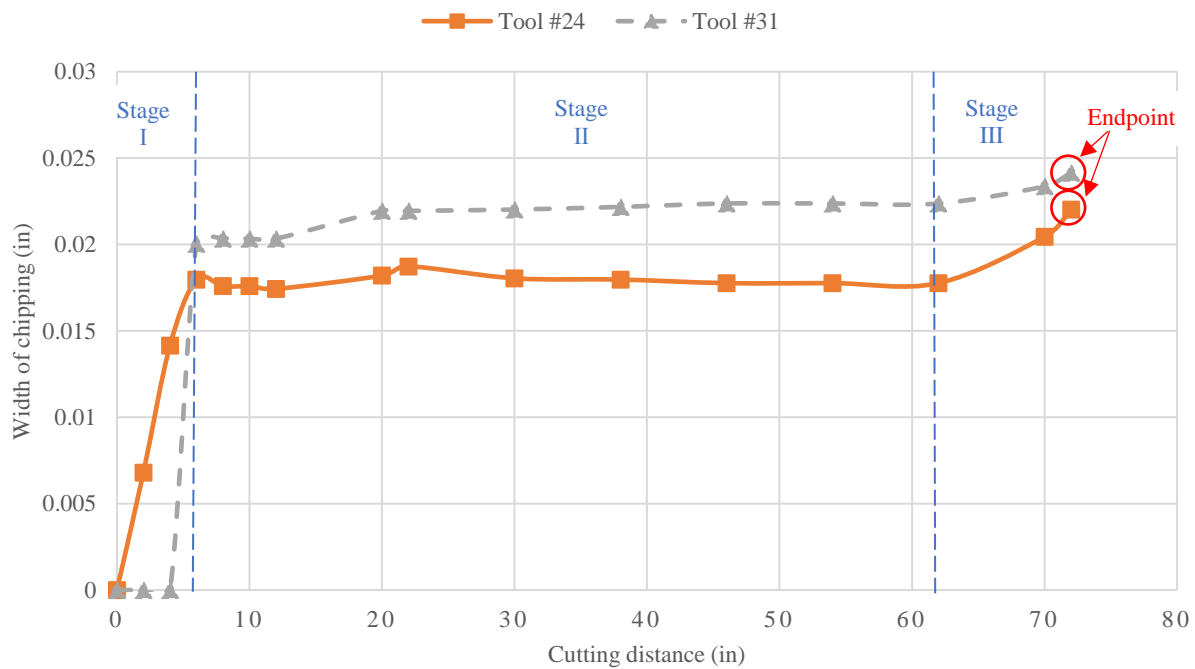


Fig. 24 The variation of chipping in long cutting distance

Three stages were found in the variation. The width of chipping increased dramatically in the first stage and kept instance in the second stage. In the second stage, the width of chipping kept instance during a long cutting distance compare to the cutting distance of the first stage. In

the third stage, the width of chipping increased again until reached the ending point.

In the first stage, since the cutting edge was sharp, and the rake angle was positive as shown in Fig. 25 (a). Only the material on the tip of cutting edge were hold the cutting force when cutting the workpiece. Therefore, the chipping appeared and extended quickly at the first stage. The cutting edge uses chipping to adjust its shape to hold the cutting force until the geometry shape is strong enough to hold the cutting force. After losing the tip of cutting edge, the rake angle of the cutting edge was negative as shown in Fig. 25 (b), and more material of the cutting edge was holding the cutting force.

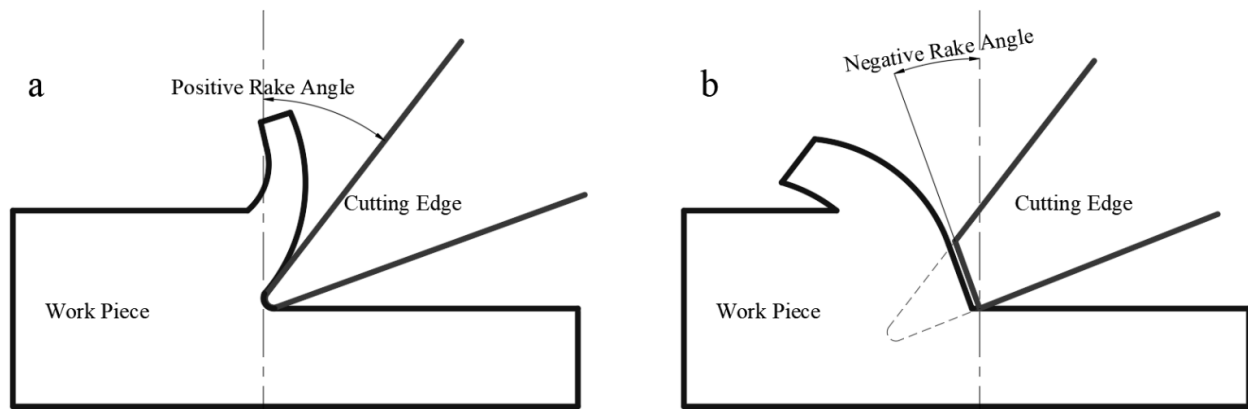


Fig. 25 (a) Cutting edge without chipping (b) cutting edge with chipping

In the second stage, the chipping did not extend after a long cutting distance. However, the cutting force increased after losing the tip because of the negative rake angle. Hence, a balance between the cutting force and the geometry of the cutting edge was built. In the following cutting process, due to the flank wear appeared on the new cutting edge, the cutting force increased gradually. Meanwhile, the low surface roughness caused by the exciting chipping also increased the cutting force. Therefore, the microcracks appeared and propagation slowly on the new cutting edge because of the cycling mechanical load [24]. The extension of the chipping in the third stage

are mainly caused by the microcracks generated in the second stage.

One of the four flutes of the milling tool # 24 in different loops are shown in Fig. 24 to explain this phenomenon. The cutting edge before the experiment are shown in Fig. 26 (a). The cutting edges in Fig. 26 (b), Fig. 26 (c), and Fig. 26 (d) are the same cutting edge after the cutting distance of 6 inches, 54 inches, and 72 inches. The chipping appeared and extended to what it looks like in Fig. 26 (b) only after cutting 6 inches of workpiece. However, comparing with the Fig. 26 (b) and Fig. 26 (c), the width of chipping did not change markedly. In other words, chipping did not extend after cutting 46 inches of workpiece. After cutting 46 inches of workpiece, the chipping extended till the cutting distance was 72 inches when the width of chipping was greater than the width of cutting zone which shown in Fig. 26 (d).

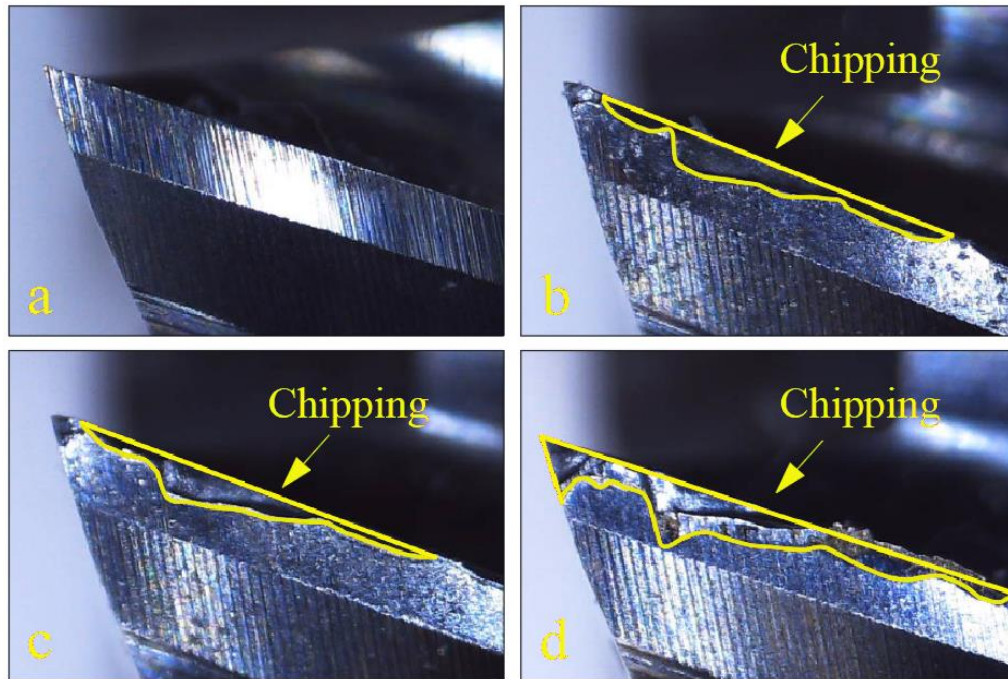


Fig. 26 (a) Tool # 24 before the experiment (b) Tool # 24 when cutting distance was 6 inches (c) Tool # 24 when cutting distance was 46 inches (d) Tool # 24 when cutting distance was 72 inches

6.4.2 The extension of the chipping in short cutting distance

Except the milling tools mentioned previously, the other milling tools used in experiments became unusable after a short cutting distance because of the high cutting force. After losing the tips of cutting edges, the rest part of cutting edges of the tool #24 and the tool #31 can still hold the cutting force in the following cutting process. However, since the low cutting speed or high chip load, the cutting force on the other milling tools was higher because and cannot be held even lost the tips of cutting edges. Therefore, the chipping appeared and extended till the width of chipping was greater than the width of cutting zone and the cutting process was stopped. In this process, the cutting edge also used chipping to adjust the geometry shape to hold the cutting force. However, the cutting force was so large that a lot of material need to be lost in order to hold the cutting force and the width of chipping was greater than width of cutting zone before the cutting edge finished the adjustment. If the width of chipping used as criteria of endpoint was wider, more milling tool might be used for longer cutting distance. Four of these milling tools are taken as instances which include tool #2, tool #6, tool #7, and tool #26. The variation of a chipping on each of these three tools are shown in Fig. 27.

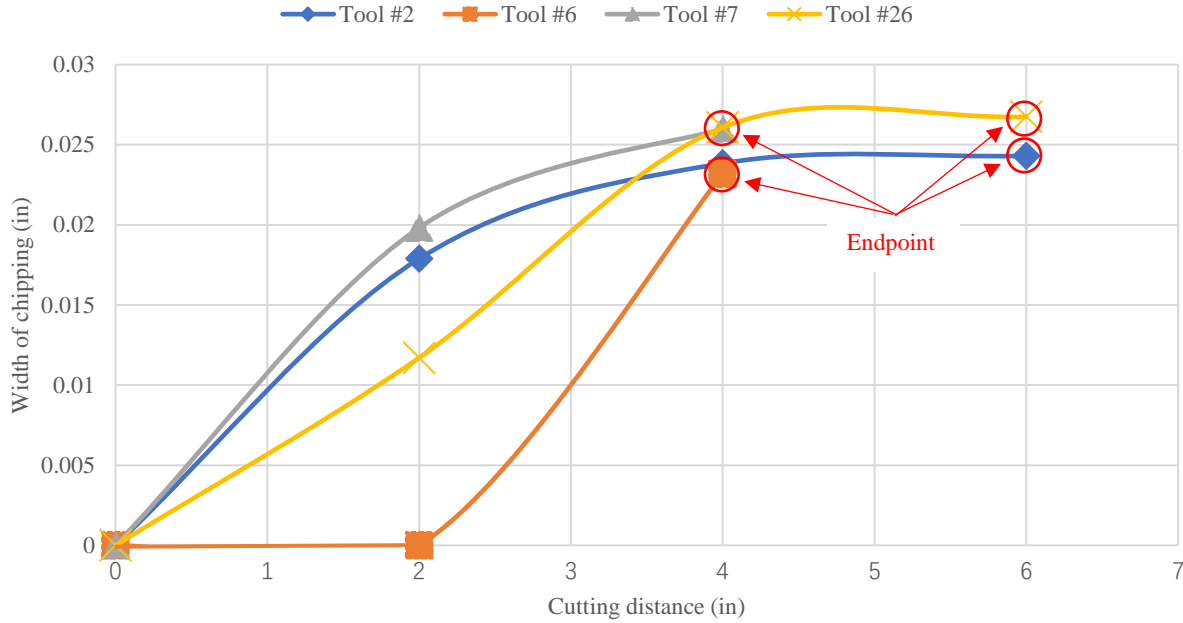


Fig. 27 The variation of chipping in short cutting distance

One of the four flutes of the milling tool # 7 in different loops are being taken as an instance and shown in Fig. 28. The cutting edges in Fig. 28 (a) and Fig. 28 (b) are the same cutting edge after the cutting distance of 2 inches and 4 inches. After cutting 2 inches of workpiece, the chipping appeared on the tool # 7 which shown in Fig. 28 (a). However, since the cutting force is so large, the cutting edge lost more material in the following cutting process to hold the cutting force. Therefore, the chipping in the Fig. 28 (a) extended to the chipping in the Fig. 28 (b).

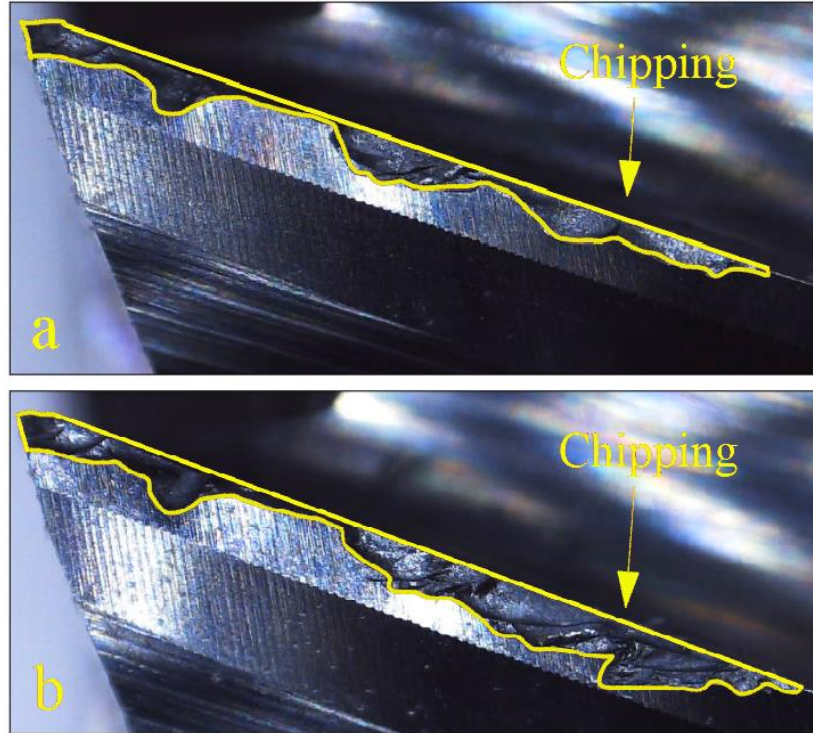


Fig. 28 (a) Tool # 7 when cutting distance was 2 inches (b) Tool # 7 when cutting distance was 4 inches

The purpose of the cutting zone used in this study is only to stop the experiment instead of failure criterion. If failure criterion of a milling tool is the width of chipping, the failure criterion should depend on the requirement of surface quality of the part and the variation of the chipping. Firstly, the chipping on the milling tool effects the surface quality of a part dramatically. Therefore, it is reasonable to decide the failure criteria of a milling tool based on the requirement of surface quality. Meanwhile, if the failure criterion of milling tool was very close to the width of chipping in the second stage, it is better to use the width of chipping in the second stage as the failure criteria. Since the width of chipping keep constant for a long cutting distance in the second stage, the milling tool can be used for a long cutting distance by using this width of chipping as failure criteria.

6.5 Mutual effect between the tool wear and chipping

It is found that the flank wear appeared when the chipping was constant during the long-distance milling process. The flank wear that appeared with chipping might lead to the extension of the chipping. Since the flank wear increased the surface roughness of the cutting edge, the cutting force was increased by the appearance and extension of the flank wear. When the cutting force was great enough that the current cutting edge with chipping could not hold, the cutting edge had to loss more material in order to hold the cutting force. Therefore, the current chipping extended, or the new chipping appeared.

As mentioned in section 6.1, the milling tool #24 cut a long distance of the workpiece with the chipping on it. The flank wear appeared on the chipping as shown in Fig. 29 (a). After cutting 6 inches of the workpiece, there was no new chipping appeared, only the existing chipping extended and shown in Fig. 29 (b). Especially, the shape of the chipping in the Fig. 29 (b) followed the shape of the flank wear in the Fig. 29 (a). Since the material at of the cutting edge where the flank wear located held the increasing cutting force, more material of this part had to be lost in order to hold the increasing cutting force.

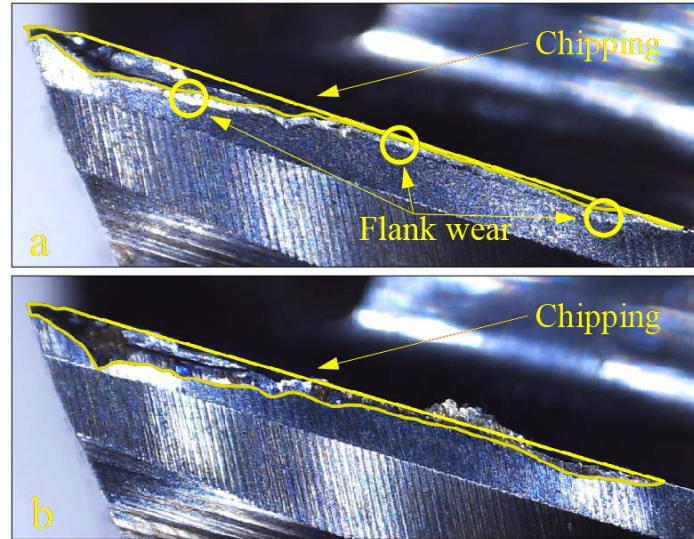


Fig. 29 (a) the chipping on the tool #24 before extending (b) the chipping on the tool#24 after extending

6.6 Usability of Taylor equation

Based on the propagation of the chipping shown in the previous section, the longest tool life was 72 in. The tool life of the most milling tools used in this study was even much shorter than 72 in. However, the tool life estimated by Taylor equation, which is based on the propagation of flank wear, is more than 90 in. Since the flank wear is caused by the friction between flank face and machined surface and the chipping is a kind of fracture, the propagation of flank wear is more gently than chipping. Consequently, if the failure criterion of the width of flank wear is same as the width of chipping, the tool life estimated by Taylor equation is longer than the tool life which uses the width of chipping as the failure criterion. Therefore, the Taylor equation cannot estimate the tool life accurately when the chipping is the dominant tool condition instead of flank wear. However, it is not mean that the propagation of chipping is totally randomly.

The tool life curves of tool #24 and tool #31 show the similar tendency of chipping propagation in three stages. Therefore, the width of chipping can be potentially estimated.

However, it is noticed that the width of chipping on these milling tools at the same stage are not same. Since the different cutting conditions caused different cutting force and the stable geometric shape under different cutting force are different, the width of chipping on the tool #24 and tool #31 are different. Therefore, more cutting conditions will be tested in order to obtain more tool life curves with all three stages of chipping propagation.

Chapter 7 Conclusions

1. Since the corner region of the milling tool does not have enough material to hold the cutting force, the chipping often occurred on this region.
2. The chipping always occurred on the depth-of-cut region of cutting edge. Part of this region cut the workpiece, however, another part did not. Therefore, the difference of cutting force between two parts of this region caused the chipping.
3. The chipping observed in this study was caused by the high cutting force. The lower RPM increased the cutting force since the temperature was not high enough to soften the workpiece and decrease the cutting force. In addition, the higher chip load per tooth also increased the cutting force since the strain hardening of the workpiece.
4. It is observed that if one flute had chipping, the other flutes had chipping at the same position since the chipping that occurred first left more material on the machined surface which increased the chip load per tooth on the following flutes.
5. There are three stages in the process of the extension of the chipping if the cutting distance was long. In the first stage, cutting edge uses the chipping to adjust the shape of itself in order to make more material to hold the cutting force. In the second stage, the width of the chipping changes minimally. However, since the appearance and the extension of the microcracks on the remaining cutting edge in the second stage, chipping extends at the third stage.
6. The flank wear was found to appear along the outline of the chipping when the chipping did not extend during a long cutting distance. The flank wear may cause the extension of chipping in the third stage because the flank wear increased the cutting force.
7. Since the mechanism and tendency of chipping propagation and flank wear propagation are different, Taylor equation cannot estimate the tool life properly when the chipping is the

dominant tool condition. However, the curves with three stages of the chipping propagation show that the width of chipping can be estimated potentially.

Chapter 8 Future Work

Future work is being proposed in the following areas:

1. Since the milling machine used in this study is for prototyping, this machine is not rigid enough and had the vibration in the milling process. Vibration also caused by the small diameter of the milling tool used in this study. The vibration increased the probability of the chipping generation. Therefore, the milling machine with higher rigidity and the milling tools with bigger diameter will be used in order to decrease the vibration and obtain the performance of the carbide milling tool closer to the performance in mass production.
2. Only two milling tools shown the tool life curve with three stages and it is hard to establish a mature model to estimate the width of chipping under different cutting conditions. Therefore, more cutting conditions will be tested in order to obtain more curves of chipping propagation with all three stages.
3. It is noticed that the chipping caused by thermal cracks was not observed since the RPM used in this research were relatively low. Therefore, higher RPM will be used in future and the chipping caused by the cyclic thermal load is hoped to be observed.
4. Since the BUE was not obvious and no crater wear was observed, the interaction between different tool conditions was not observed clearly and analyzed. Since different tool conditions occur under different cutting conditions, more cutting conditions will be tested. Meanwhile, more tool conditions and the interaction among them are hoped to be studied.

Appendix A: Chemical composition of 1020 steel

Element	Content
Carbon, C	0.17 - 0.230 %
Iron, Fe	99.08 - 99.53 %
Manganese, Mn	0.30 - 0.60 %
Phosphorous, P	≤ 0.040 %
Sulfur, S	≤ 0.050 %

Appendix B: Mechanical properties of 1020 steel

Mechanical Properties	Metric	Imperial
Hardness, Brinell	111	111
Hardness, Knoop (Converted from Brinell hardness)	129	129
Hardness, Rockwell B (Converted from Brinell hardness)	64	64
Hardness, Vickers (Converted from Brinell hardness)	115	115
Tensile Strength, Ultimate	394.72 MPa	57249 psi
Tensile Strength, Yield	294.74 MPa	42748 psi
Elongation at Break (in 50 mm)	36.5 %	36.5 %
Reduction of Area	66.0 %	66.0 %
Modulus of Elasticity (Typical for steel)	200 GPa	29000 ksi
Bulk Modulus (Typical for steel)	140 GPa	20300 ksi
Poissons Ratio	0.290	0.290
Izod Impact	125 J	92.2 ft-lb
Shear Modulus (Typical for steel)	80.0 GPa	11600 ksi

Appendix C: Cutting conditions used in this study

No.	RPM	Chip Load (in)	Feed Rate (in/min)
1	100	0.0008	0.3
2	800	0.0008	2.6
3	2000	0.0008	6.4
4	100	0.0015	0.6
5	800	0.0015	4.8
6	1200	0.0015	7.2
7	100	0.0022	0.9
8	400	0.0022	3.5
9	800	0.0022	7.0
10	100	0.003	1.2
11	400	0.003	4.8
12	1200	0.0008	3.8
13	400	0.0015	2.4
14	1400	0.0015	8.4
15	1200	0.0022	10.6
16	800	0.003	9.6
17	150	0.0022	1.3
18	400	0.0038	6.1
19	800	0.0038	12.2
20	1400	0.0022	12.3
21	600	0.0022	5.3

No.	RPM	Chip Load (in)	Feed Rate (in/min)
22	1200	0.003	14.4
23	200	0.003	2.4
24	2400	0.0008	7.7
25	1000	0.0008	3.2
26	600	0.0015	3.6
27	1400	0.0015	8.4
28	1200	0.0038	18.2
29	800	0.0046	14.7
30	1400	0.003	16.8
31	2200	0.0008	7.0
32	1200	0.0046	22.1
33	2300	0.0008	7.4
34	900	0.0008	2.9
35	1300	0.0015	7.8
36	1300	0.0022	11.4
37	1300	0.003	15.6
38	700	0.0015	4.2
39	700	0.0022	6.2
40	300	0.003	3.6
41	1000	0.0038	15.2
42	600	0.0038	9.1

Appendix D: Cutting distance used in each loop

Stages		Cutting distance (in)	Stages		Cutting distance (in)
Initial stage		2	Follow-up stage	Loop 8	2
Follow-up stage	Loop 1	2		Loop 9	8
	Loop 2	2		Loop 10	8
	Loop 3	2		Loop 11	8
	Loop 4	2		Loop 12	8
	Loop 5	2		Loop 13	8
	Loop 6	4		Loop 14	8
	Loop 7	4		Loop 15	2

Appendix E: Results of observation in initial stage

Tool number	Tool conditions and size	
	Maximum width of flank wear (in)	Maximum width of chipping (in)
1	0.0008	0
2	0.0008	0.0179
3	0.0007	0.0021
4	0.0004	0.0214
5	0.0015	0
6	0.0018	0
7	0	0.0198
8	0.0006	0.0180
9	0.0005	0
10	0	0.0241
11	0.0008	0
12	0.0008	0.0179
13	0.0008	0.0181
14	0	0.0258
15	0.0023	0
16	0.0008	0
17	0.0005	0.0262
18	0.0004	0.0266
19	0.0002	0
20	0.0003	0.0121
21	0	0.0107

22	0.0004	0
23	0.0002	0
24	0.0003	0.0068
25	0.0005	0
26	0	0.0117
27	0	0.0362
28	0.0003	0.0591
29	0.0003	0.0473
30	0	0.0862
31	0.0009	0
32	0.0004	0.0241

Appendix F-1: Results of observation in the first loop of follow-up stage

Tool number	Tool conditions and size	
	Maximum width of flank wear (in)	Maximum width of chipping (in)
1	0.0011	0.0140
2	0.0009	0.0238
3	0.0011	0.0245
4	0.0006	0.0205
5	0.0015	0
6	0.0012	0
7	0	0.0260
8	0.0006	0.0167
9	0.0009	0
11	0.0011	0
12	0.0009	0.0196
13	0.0009	0.0206
15	0.0023	0.0233
16	0.0008	0
17	0.0005	0.0262
19	0.0006	0.0211
21	0	0.0164
22	0.0008	0.0244
23	0.0008	0.0208

24	0.0003	0.0141
25	0.0012	0
26	0	0.0261
31	0.0009	0

Appendix F-2: Results of observation in the second loop of follow-up stage

Tool number	Tool conditions and size	
	Maximum width of flank wear (in)	Maximum width of chipping (in)
1	0.0015	0.015
2	0.0013	0.0238
3	0.0011	0.0245
5	0.0015	0
6	0.0012	0
9	0.0009	0
11	0.0011	0
12	0.0009	0.0217
13	0.0009	0.0206
15	0.0023	0.0233
16	0.0008	0.0231
22	0.0008	0.0244
24	0.0003	0.0180
25	0.0012	0.0039
26	0	0.0267
31	0.0011	0.0200

Appendix F-3: Results of observation in the third loop of follow-up stage

Tool number	Tool conditions and size	
	Maximum width of flank wear (in)	Maximum width of chipping (in)
1	0.0016	0.0212
2	0.0013	0.0244
3	0.0011	0.0262
5	0.0015	0.0201
6	0.0012	0
9	0.0009	0.0211
11	0.0011	0.0186
12	0.0009	0.0222
13	0.0009	0.0209
15	0.0023	0.0240
24	0.0003	0.0180
25	0.0012	0.0039
26	0	0.0269
31	0.0012	0.0203

Appendix F-4: Results of observation in the forth loop of follow-up stage

Tool number	Tool conditions and size	
	Maximum width of flank wear (in)	Maximum width of chipping (in)
3	0.0011	0.0262
6	0.0012	0.0231
9	0.0009	0.0211
15	0.0023	0.0241
24	0.0003	0.0180
31	0.0015	0.0203

Appendix F-5: Results of observation in the fifth loop of follow-up stage

Tool number	Tool conditions and size	
	Maximum width of flank wear (in)	Maximum width of chipping (in)
3	0.0011	0.0262
6	0.0015	0.0231
9	0.0009	0.0211
15	0.0023	0.0241
24	0.0003	0.0180
31	0.0015	0.0203

Appendix F-6: Results of observation in the sixth loop of follow-up stage

Tool number	Tool conditions and size	
	Maximum width of flank wear (in)	Maximum width of chipping (in)
3	0.0011	0.0262
6	0.0015	0.0254
9	0.0009	0.0211
15	0.0023	0.0241
24	0.0003	0.0180
31	0	0.0214

Appendix F-7: Results of observation in the seventh loop of follow-up stage

Tool number	Tool conditions and size	
	Maximum width of flank wear (in)	Maximum width of chipping (in)
9	0	0.0217
15	0.0023	0.0241
24	0	0.0182
31	0.0015	0.0214

Appendix F-8: Results of observation in the eighth loop of follow-up stage

Tool number	Tool conditions and size	
	Maximum width of flank wear (in)	Maximum width of chipping (in)
9	0	0.0231
15	0.0023	0.0241
24	0	0.0187
31	0.0015	0.0214

Appendix F-9: Results of observation in the ninth loop of follow-up stage

Tool number	Tool conditions and size	
	Maximum width of flank wear (in)	Maximum width of chipping (in)
9	0	0.0231
15	0	0.0257
24	0	0.0187
31	0	0.0220

Appendix F-10: Results of observation in the tenth loop of follow-up stage

Tool number	Tool conditions and size	
	Maximum width of flank wear (in)	Maximum width of chipping (in)
9	0	0.0232
15	0	0.0257
24	0	0.0187
31	0	0.0222

Appendix F-11: Results of observation in the eleventh loop of follow-up stage

Tool number	Tool conditions and size	
	Maximum width of flank wear (in)	Maximum width of chipping (in)
9	0	0.0235
24	0	0.0187
31	0	0.0222

Appendix F-12: Results of observation in the twelfth loop of follow-up stage

Tool number	Tool conditions and size	
	Maximum width of flank wear (in)	Maximum width of chipping (in)
9	0	0.0248
24	0	0.0187
31	0	0.0224

Appendix F-13: Results of observation in the thirteenth loop of follow-up stage

Tool number	Tool conditions and size	
	Maximum width of flank wear (in)	Maximum width of chipping (in)
24	0	0.0187
31	0	0.0224

Appendix F-14: Results of observation in the fourteenth loop of follow-up stage

Tool number	Tool conditions and size	
	Maximum width of flank wear (in)	Maximum width of chipping (in)
24	0	0.0204
31	0	0.0234

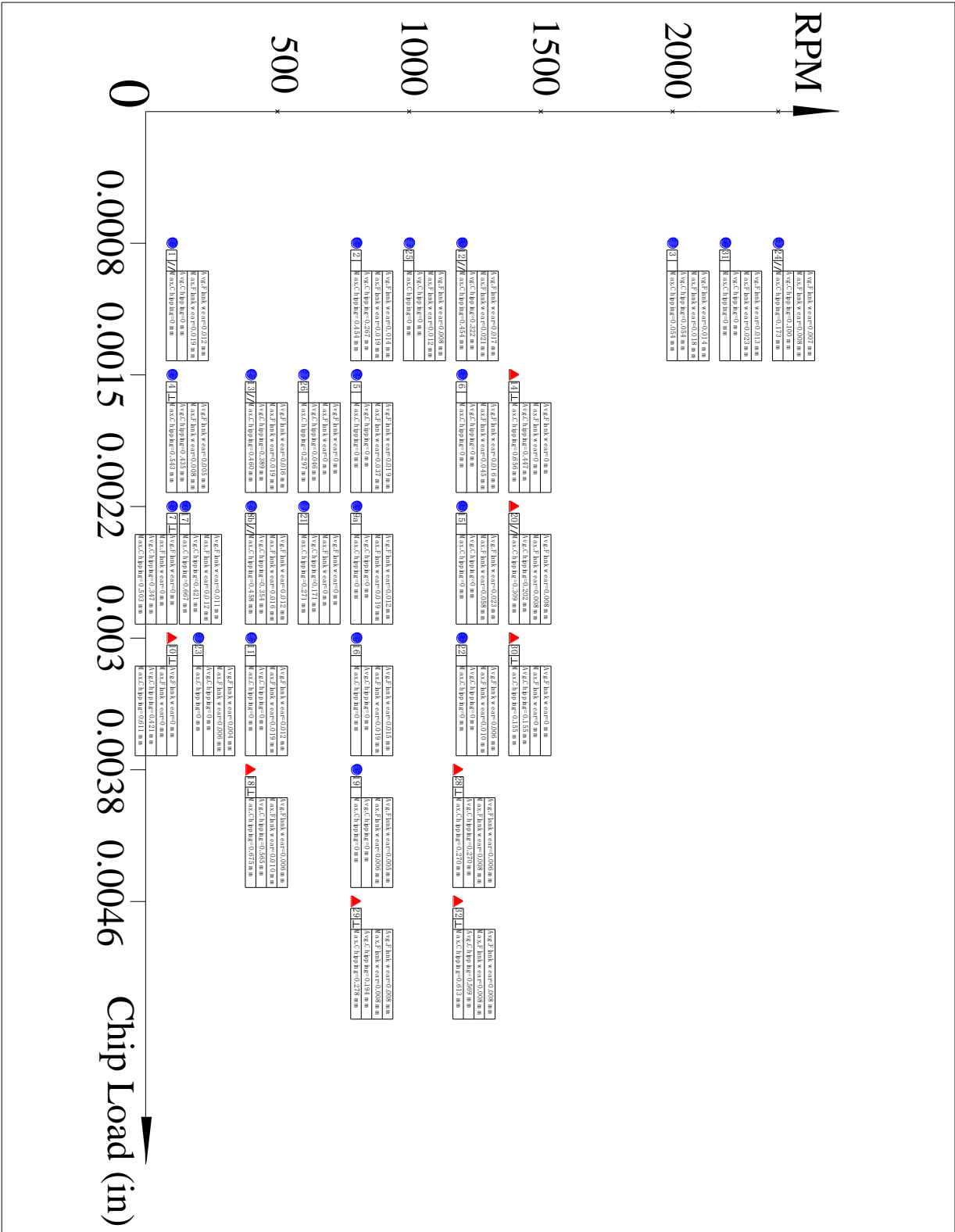
Appendix F-15: Results of observation in the fifteenth loop of follow-up stage

Tool number	Tool conditions and size	
	Maximum width of flank wear (in)	Maximum width of chipping (in)
24	0	0.0220
31	0	0.0241

Appendix F-16: Results of observation in the sixteenth loop of follow-up stage

Tool number	Tool conditions and size	
	Maximum width of flank wear (in)	Maximum width of chipping (in)
24	0	0.0221
31	0	0.0242

Appendix G: An example of the map



Reference

- [1] S.-L. Chen and Y. W. Jen, "Data fusion neural network for tool condition monitoring in CNC milling machining," *Int. J. Mach. Tools Manuf.*, vol. 40, no. 3, pp. 381–400, 2000.
- [2] A. J. Vallejo, R. Morales-menéndez, and J. R. Alique, "On-line Cutting Tool Condition Monitoring in Machining Processes using Artificial Intelligence," *Robot. Autom. Control*, no. October, pp. 144–166, 2008.
- [3] G. Byrne, D. Dornfeld, I. Inasaki, G. Ketteler, W. König, and R. Teti, "Tool Condition Monitoring (TCM) - The Status of Research and Industrial Application," *CIRP Ann. - Manuf. Technol.*, vol. 44, no. 2, pp. 541–567, 1995.
- [4] J. . Stephenson, D.A dan Agapiou, *Metal Cutting theory and Stephenson, D.A dan Agapiou, J. . (1996). Metal Cutting theory and practice. CRC Press. practice. CRC Press, 1996.*
- [5] N. Fang and P. Dewhurst, "Slip-line modeling of built-up edge formation in machining," *Int. J. Mech. Sci.*, vol. 47, no. 7, pp. 1079–1098, 1968.
- [6] ISO, "ISO 8688-2 Tool Life Testing in Milling - Part 2: End Milling," *International Standards*. 1989.
- [7] S. Zhang, J. F. Li, and Y. W. Wang, "Tool life and cutting forces in end milling Inconel 718 under dry and minimum quantity cooling lubrication cutting conditions," *J. Clean. Prod.*, vol. 32, pp. 81–87, 2012.
- [8] A. Jawaid, C. H. Che-Haron, and A. Abdullah, "Tool wear characteristics in turning of titanium alloy Ti-6246," *J. Mater. Process. Technol.*, vol. 92–93, pp. 329–334, 1999.
- [9] D. E. D. Snr., "Sensor signals for tool-wear monitoring in metal cutting operations - a review of methods," *Int. J. Mach. Tools Manuf.*, vol. 40, no. 8, pp. 1073–1098, 2000.
- [10] D. Axinte and N. Gindy, "Assessment of the effectiveness of a spindle power signal for tool condition monitoring in machining processes," *Int. J. Prod. Res.*, vol. 42, no. 13, pp. 2679–2691, 2004.
- [11] X. Q. Chen and H. Z. Li, "Development of a tool wear observer model for online tool condition monitoring and control in machining nickel-based alloys," *Int. J. Adv. Manuf. Technol.*, vol. 45, no. 7–8, pp. 786–800, 2009.
- [12] T. Childs, "Metal Machining Theory and Applications."
- [13] Kharagpur, "Failure of cutting tools and tool life," .
- [14] M. Alauddin and M. A. El Baradie, "Tool life model for end milling steel (190 BHN)," *J. Mater. Process. Technol.*, vol. 68, no. 1, pp. 50–59, 1997.

- [15] P. Chakraborty, "Tool Life and Flank Wear Modeling of Physical Vapour Deposited TiAlN/TiN Multilayer Coated Carbide End Mill Inserts when Machining 4340 Steel Under Dry and Semi-Dry Cutting Conditions," *PhD thesis*, no. December, 2007.
- [16] A. L. B. Dos Santos, M. A. V. Duarte, A. M. Abrão, and A. R. Machado, "An optimisation procedure to determine the coefficients of the extended Taylor's equation in machining," *Int. J. Mach. Tools Manuf.*, vol. 39, no. 1, pp. 17–31, 1999.
- [17] M. S. J. H. M. Alauddin, M.A. El Baradie, "Tool-life testing in the end milling of Inconel 718," *Mater. Process. Technol.*, vol. 55, pp. 321–330, 1994.
- [18] J. Gu, G. Barber, S. Tung, and R.-J. Gu, "Tool life and wear mechanism of uncoated and coated milling inserts," *Wear*, vol. 225–229, pp. 273–284, 1999.
- [19] G. E. D'Errico, "Tool-life reliability of cermet inserts in milling tests," *J. Mater. Process. Technol.*, vol. 77, pp. 337–343, 1998.
- [20] A. E. Diniz and J. C. Filho, "Influence of the relative positions of tool and workpiece on tool life, tool wear and surface finish in the face milling process," *Wear*, vol. 232, no. 1, pp. 67–75, 1999.
- [21] Z. G. Wang, Y. S. Wong, and M. Rahman, "High-speed milling of titanium alloys using binderless CBN tools," *Int. J. Mach. Tools Manuf.*, vol. 45, no. 1, pp. 105–114, 2005.
- [22] K. Kudou, T. Ono, and S. Okada, "Crater wear characteristics of an Fe-diffused carbide cutting tool," *J. Mater. Process. Technol.*, vol. 132, no. 1–3, pp. 255–261, 2003.
- [23] P. Palanisamy, I. Rajendran, and S. Shanmugasundaram, "Prediction of tool wear using regression and ANN models in end-milling operation a critical review," *Int. J. Adv. Manuf. Technol.*, vol. 37, no. 7–8, pp. 29–41, 2008.
- [24] Z. Q. Liu, X. Ai, H. Zhang, Z. T. Wang, and Y. Wan, "Wear patterns and mechanisms of cutting tools in high-speed face milling," *J. Mater. Process. Technol.*, vol. 129, no. 1–3, pp. 222–226, 2002.
- [25] Ezugwu, E.O, Wang, Z.M., and Machado, A.R., "The machinability of nickel-based alloys : a review," *J. Mater. Process. Technol.*, vol. 86, no. 1–3, pp. 1–16, 1998.
- [26] M. Nordin, R. Sundström, T. I. Selinder, and S. Hogmark, "Wear and failure mechanisms of multilayered PVD TiN/TaN coated tools when milling austenitic stainless steel," *Surf. Coatings Technol.*, vol. 133–134, pp. 240–246, 2000.
- [27] A. Li, J. Zhao, D. Wang, J. Zhao, and Y. Dong, "Failure mechanisms of a PCD tool in high-speed face milling of Ti-6Al-4V alloy," *Int. J. Adv. Manuf. Technol.*, vol. 67, no. 9–12, pp. 1959–1966, 2013.
- [28] G. J. Wolfe, C. J. Petrosky, and D. T. Quinto, "The role of hard coatings in carbide milling tools," *J. Vac. Sci. Technol. A Vacuum, Surfaces, Film.*, vol. 4, no. 6, pp. 2747–2754, 1986.

- [29] D. Zhu, X. Zhang, and H. Ding, "Tool wear characteristics in machining of nickel-based superalloys," *Int. J. Mach. Tools Manuf.*, vol. 64, pp. 60–77, 2013.
- [30] A. Jawaid, S. Sharif, and S. Koksai, "Evaluation of wear mechanisms of coated carbide tools when face milling titanium alloy," *J. Mater. Process. Technol.*, vol. 99, no. 1, pp. 266–274, 2000.
- [31] S. A.T., Q. D.T., and G. G.P., "Comparison of the steel-milling performance of carbide inserts with MTCVD and PVD TiCN coatings," *Int. J. Refract. Met. Hard Mater.*, vol. 14, no. 1–3 SPEC. ISS., pp. 31–40, 1996.
- [32] H. Li, G. He, X. Qin, G. Wang, C. Lu, and L. Gui, "Tool wear and hole quality investigation in dry helical milling of Ti-6Al-4V alloy," *Int. J. Adv. Manuf. Technol.*, vol. 71, no. 5–8, pp. 1511–1523, 2014.
- [33] A. Jawaid, S. Koksai, and S. Sharif, "Cutting performance and wear characteristics of PVD coated and uncoated carbide tools in face milling Inconel 718 aerospace alloy," *Journal of Materials Processing Technology*, vol. 116, no. 1, pp. 2–9, 2001.
- [34] S. Saketi, S. Sveen, S. Gunnarsson, R. M'Saoubi, and M. Olsson, "Wear of a high cBN content PCBN cutting tool during hard milling of powder metallurgy cold work tool steels," *Wear*, vol. 332–333, pp. 752–761, 2015.
- [35] Y. Su, N. He, L. Li, and X. L. Li, "An experimental investigation of effects of cooling/lubrication conditions on tool wear in high-speed end milling of Ti-6Al-4V," *Wear*, vol. 261, no. 7–8, pp. 760–766, 2006.
- [36] D. K. Baek, T. J. Ko, and H. S. Kim, "Real time monitoring of tool breakage in a milling operation using a digital signal processor," *J. Mater. Process. Technol.*, vol. 100, no. 1, pp. 266–272, 2000.
- [37] A. Sharman, R. C. Dewes, and D. K. Aspinwall, "Tool life when high speed ball nose end milling Inconel 718TM," *Journal of Materials Processing Technology*, vol. 118, no. 1–3, pp. 29–35, 2001.